Analysis of Compatible Discrete Operator Schemes for the Stokes Equations on Polyhedral Meshes

Jérôme Bonelle, Alexandre Ern

Analysis of Compatible Discrete Operator Schemes for the Stokes Equations on Polyhedral Meshes

Jerome Bonelle
EDF R&D
6, quai Watier, BP 49
78401 Chatou cedex
jerome.bonelle@edf.fr

Alexandre Ern
Université Paris-Est, CERMICS
Ecole des Ponts ParisTech
77455 Marne la Vallée Cedex 2, France
ern@cermics.enpc.fr

August 1, 2014

Abstract

Compatible Discrete Operator schemes preserve basic properties of the continuous model at the discrete level. They combine discrete differential operators that discretize exactly topological laws and discrete Hodge operators that approximate constitutive relations. We devise and analyze two families of such schemes for the Stokes equations in curl formulation, with the pressure degrees of freedom located at either mesh vertices or cells. The schemes ensure local mass and momentum conservation. We prove discrete stability by establishing novel discrete Poincaré inequalities. Using commutators related to the consistency error, we derive error estimates with first-order convergence rates for smooth solutions. We analyze two strategies for discretizing the external load, so as to deliver tight error estimates when the external load has a large curl-free or divergence-free part. Finally, numerical results are presented on three-dimensional polyhedral meshes.

1 Introduction

Compatible Discrete Operator (CDO) schemes belong to the broad class of compatible or mimetic schemes, which preserve basic properties of the continuous model at the discrete level; see [3, 4, 9, 14, 16, 18, 22, 30, 35, 38, 42, 44] and references therein. Following the seminal ideas of [43] and [12], the degrees of freedom (DoFs) are defined using de Rham maps, and their localization results from the physical nature of the fields. Moreover, a distinction is operated between topological laws (that are discretized exactly) and constitutive relations (that are approximated). CDO schemes are formulated using discrete differential operators for the topological laws and discrete Hodge operators for the constitutive relations. The discrete differential operators produce a cochain complex and they commute with the de Rham maps. The discrete Hodge operator is the key operator in the CDO framework. The design of this operator is not unique, and each design leads to a specific scheme [see 41, 31, 11]. CDO schemes involve two meshes: a primal mesh (the only one seen by the end-user) and a dual mesh. The discrete Hodge operator links DoFs defined on the primal mesh to DoFs defined on the dual mesh. Moreover, discrete adjunction properties hold for discrete differential operators on the primal and dual mesh. In [11], CDO schemes have been analyzed for elliptic problems on polyhedral meshes.

The Stokes equations model flows of incompressible and viscous fluids where the advective inertial forces are negligible with respect to the viscous forces. In this paper, we focus on the stationary Stokes equations posed on an open, bounded and connected domain $\Omega \subset \mathbb{R}^3$ with boundary $\partial\Omega$ and outward normal $\underline{\nu}_{\partial\Omega}$. Our starting point is to formulate the viscous stresses in the momentum balance using the curl operator. This way, all the terms in the Stokes equations can be interpreted using scalar-valued differential forms. We analyze two formulations. The first one, hereafter called 2-field curl formulation,

takes the form

$$\begin{cases} \underline{\mathrm{curl}}(\underline{\mathrm{curl}}(\underline{u})) + \underline{\mathrm{grad}}(p) &= \underline{f}, \qquad \text{in } \Omega, \\ \mathrm{div}(\underline{u}) &= 0, \qquad \text{in } \Omega, \end{cases} \tag{1}$$

where $\underline{u}$ is the velocity, p the pressure, and $\underline{f}$ the external load. Introducing the vorticity $\underline{\omega} := \underline{\mathrm{curl}}\,\underline{u}$, the second formulation, hereafter called 3-field curl formulation (also called Velocity-Vorticity-Pressure formulation in the literature), takes the form

$$\begin{cases} -\underline{\omega} + \underline{\mathrm{curl}}(\underline{u}) &= \underline{0}, \qquad \text{in } \Omega, \\ \underline{\mathrm{curl}}(\underline{\omega}) + \underline{\mathrm{grad}}(p) &= \underline{f}, \qquad \text{in } \Omega, \\ \mathrm{div}(\underline{u}) &= 0, \qquad \text{in } \Omega. \end{cases} \tag{2}$$

Essential and natural boundary conditions (BCs) can be considered for both formulations. The first set of BCs enforces the value of the normal component of the velocity $\underline{u} \cdot \underline{\nu}_{\partial\Omega}$ and that of the tangential components of the vorticity $\underline{\omega} \times \underline{\nu}_{\partial\Omega}$ at the boundary. These BCs are natural for (1) and essential for (2). As the pressure is then determined up to an additive constant, the additional requirement of p having zero mean-value is typically added. The second set of BCs enforces the value of the tangential components of the velocity $\underline{u} \times \underline{\nu}_{\partial\Omega}$ and the value of the pressure at the boundary. These BCs are essential for (1) and natural for (2). Curl formulations of the Stokes equations have been considered, e.g., by [37] and [25, 26] for the 3-field curl formulation and by [13] for the 2-field curl formulation.

In the present work, we devise and analyze CDO schemes for the Stokes problem in the curl formulations (1) and (2). Since the pressure plays the role of a potential, its DoFs are located at primal or dual mesh vertices. The former case hinges on (1) leading to vertex-based pressure schemes, while the latter hinges on (2) leading to cell-based pressure schemes (since primal cells are in one-to-one correspondence with dual mesh vertices). Both CDO schemes involve two discrete Hodge operators, one linking the velocity (seen as a circulation) to the mass flux and the other linking the vorticity to the viscous stress. The present CDO schemes feature several interesting properties. They can be deployed on polyhedral meshes, and the discrete solution satisfies local mass and momentum conservation. Another benefit from the CDO framework is to deliver two possible discretizations of the external load. This issue is quite important in practice so as to obtain tight error estimates when the external load has a large curl-free or a large divergence-free part (see [34] for a related work on classical Finite Element (FE) schemes and loads with a large curl-free part). In CDO schemes, both situations can be handled by simply choosing a discretization of the external load on primal or dual mesh entities, without using explicitly any Hodge–Helmholtz decomposition of the external load.

The present CDO schemes are, to our knowledge, new on polyhedral meshes, and so is the idea of considering two possible discretizations of the external load. On specific meshes, previous schemes can be recovered from the present CDO schemes. On simplicial meshes and using Whitney forms to build the discrete Hodge operator, the present vertex-based (resp., cell-based) pressure schemes yield the recent FE scheme by [1] (resp., by [37] and [25, 26]). On Delaunay–Voronoï meshes where diagonal discrete Hodge operators can be used, the present CDO schemes are closely related to the recent MAC schemes by [27] on triangular meshes; see also [39]. Furthermore, the present cell-based pressure schemes share the same algebraic structure (same discrete differential operators, but different discrete Hodge operators) as the recent Mimetic Spectral Element method on general quadrilateral/hexahedral meshes analyzed by [32]; see also [8]. We also mention the Discrete Duality Finite Volume (DDFV) scheme on general 2D meshes by [21], which also hinges on the 3-field formulation (2).

The numerical analysis of the present CDO schemes entails some novelties. The most salient one are new Poincaré inequalities for the discrete gradient and curl operators. Similar inequalities have been derived by [4] in a conforming setting where the discrete functions belong to the functional spaces where the continuous Poincaré inequalities hold, e.g., $H^1(\Omega)$ and $H(\underline{\mathrm{curl}};\Omega)$. The difference is that the present inequalities are stated on the spaces of DoFs (and not on discrete functions) and, more importantly, that the orthogonality is stated using a discrete Hodge operator; even if this operator is devised from local reconstruction functions, the latter need not be conforming. Once these discrete Poincaré inequalities are established, the stability analysis proceeds along fairly classical lines [15, 26], which are adapted here

to the CDO framework. Furthermore, we prove *a priori* error estimates with first-order convergence rates for smooth solutions. In the first step of the proof, extending ideas from [12, 31] to the Stokes equations, we bound the error by the consistency error, the latter being expressed as a commutator involving the two discrete Hodge operators for the Stokes equations. In the second step, we proceed as in [11] to estimate the consistency error using polynomial approximation in Sobolev spaces. Another novel feature of the convergence analysis is to introduce two possible discretizations of the external load since they lead to substantially different error bounds.

The more classical formulation of the Stokes equations uses the vector Laplacian of the velocity in the momentum balance. Various schemes were proposed to discretize this formulation on polygonal or polyhedral meshes, including Mixed Finite Volumes by [24], Mimetic Finite Differences (MFD) by [5, 6] and [7], DDFV by [33], an extension of the Crouzeix–Raviart finite element by [23], and a scheme on triangular meshes based on Finite Element Exterior Calculus (FEEC) by [29]. Discretizing the vector Laplacian with CDO schemes is the subject of ongoing work.

This paper is organized as follows. In Section 2, we briefly recall the CDO framework. Then, we present and analyze vertex- and cell-based pressure CDO schemes for the Stokes equations in Sections 3 and 4, respectively. Finally, we present numerical results in Section 5. For simplicity, we often assume in what follows that Ω is simply connected and that its boundary $\partial\Omega$ is connected. Whenever needed, we refer to this assumption as $(\mathbf{H_\Omega})$.

2 The CDO Framework

2.1 Meshes and degrees of freedom

The discretization of the domain $\Omega \subset \mathbb{R}^3$ relies on a primal mesh $\mathrm{M} = \{\mathrm{V}, \mathrm{E}, \mathrm{F}, \mathrm{C}\}$, where V collects primal vertices (or 0-cells) generically denoted v, E primal edges (or 1-cells) e, F primal faces (or 2-cells) f, and C primal cells (or 3-cells) c. The primal mesh has the structure of a cellular complex, in the sense that the boundary of a k-cell in M, $1 \le k \le 3$, can be decomposed into $(k-1)$-cells belonging to M [17]. The spaces of DoFs are denoted $\mathcal{V}, \mathcal{E}, \mathcal{F}, \mathcal{C}$ and are defined as the codomains of de Rham maps acting as follows:

$$\forall \mathrm{v} \in \mathrm{V}, \quad (\mathsf{R}_{\mathcal{V}}(p))_{\mathrm{v}} := p(\mathrm{v}), \qquad \forall \mathrm{e} \in \mathrm{E}, \quad (\mathsf{R}_{\mathcal{E}}(\underline{u}))_{\mathrm{e}} := \int_{\mathrm{e}} \underline{u} \cdot \underline{\tau}_{\mathrm{e}}, \tag{3a}$$

$$\forall \mathrm{f} \in \mathrm{F}, \quad (\mathsf{R}_{\mathcal{F}}(\underline{\phi}))_{\mathrm{f}} := \int_{\mathrm{f}} \underline{\phi} \cdot \underline{\nu}_{\mathrm{f}}, \qquad \forall \mathrm{c} \in \mathrm{C}, \quad (\mathsf{R}_{\mathcal{C}}(s))_{\mathrm{c}} := \int_{\mathrm{c}} s, \tag{3b}$$

where $\underline{\tau}_{\mathrm{e}}$ is a unit tangent vector to the edge e and $\underline{\nu}_{\mathrm{f}}$ is a unit normal vector to the face f. The orientation of $\underline{\tau}_{\mathrm{e}}$ and that of $\underline{\nu}_{\mathrm{f}}$ is arbitrary, but fixed once and for all (more precisely, the orientation of f is fixed and determines the orientation of $\underline{\nu}_{\mathrm{f}}$). The definitions (3) are in agreement with the underlying physical nature of fields: a scalar potential field is discretized at vertices, a circulation at edges, a flux at faces, and a density at cells. The domain of the de Rham maps can be specified using Sobolev spaces. Fixing a real number $p \in [1, \infty]$ and taking $s_k > \frac{3-k}{p}$ for all $0 \le k \le 2$, one possibility is to require that $p \in W^{s_0,p}(\Omega)$, $\underline{u} \in W^{s_1,p}(\Omega)^3$, $\underline{\phi} \in W^{s_2,p}(\Omega)^3$, and $s \in L^p(\Omega)$; it is also possible to use (broken) Sobolev spaces [36, 45].

In addition to the primal mesh, we introduce a dual mesh $\widetilde{\mathrm{M}} := \{\widetilde{\mathrm{V}}, \widetilde{\mathrm{E}}, \widetilde{\mathrm{F}}, \widetilde{\mathrm{C}}\}$, where $\widetilde{\mathrm{V}}$ collects dual vertices generically denoted $\tilde{\mathrm{v}}$, $\widetilde{\mathrm{E}}$ dual edges $\tilde{\mathrm{e}}$, $\widetilde{\mathrm{F}}$ dual faces $\tilde{\mathrm{f}}$, and $\widetilde{\mathrm{C}}$ dual cells $\tilde{\mathrm{c}}$. There are several ways to build a dual mesh, for instance using Voronoï diagrams or a barycentric subdivision [see 11]. The precise way $\widetilde{\mathrm{M}}$ is built is not needed at this stage. We only require that there is a one-to-one correspondence between primal vertices and dual cells, primal edges and dual faces, primal faces and dual edges, and primal cells and dual vertices. As a result, $\#\widetilde{\mathrm{V}} = \#\mathrm{C}$, $\#\widetilde{\mathrm{E}} = \#\mathrm{F}$, $\#\widetilde{\mathrm{F}} = \#\mathrm{E}$ and $\#\widetilde{\mathrm{C}} = \#\mathrm{V}$, where $\#\mathrm{X}$ denotes the cardinality of the set X. To stress this one-to-one pairing, we denote $\tilde{\mathrm{v}}(\mathrm{c}) \in \widetilde{\mathrm{V}}$ the dual vertex related to the primal cell $\mathrm{c} \in \mathrm{C}$, $\tilde{\mathrm{e}}(\mathrm{f}) \in \widetilde{\mathrm{E}}$ the dual edge related to the primal

face $f \in F$, $\tilde{f}(e) \in \widetilde{F}$ the dual face related to the primal edge $e \in E$, and $\tilde{c}(v) \in \widetilde{C}$ the dual cell related to the primal vertex $v \in V$. The de Rham maps on the dual mesh act similarly to (3), with codomains denoted $\widetilde{\mathcal{V}}, \widetilde{\mathcal{E}}, \widetilde{\mathcal{F}}, \widetilde{\mathcal{C}}$. The orientation of the unit vector $\underline{\tau}_{\tilde{e}(f)}$ is determined by $\underline{\nu}_f$ for all $f \in F$ and that of $\underline{\nu}_{\tilde{f}(e)}$ by $\underline{\tau}_e$ for all $e \in E$. This means that we operate a transfer of orientation from the primal mesh to the dual mesh. Figure 1 illustrates primal and dual mesh entities. Contrary to the primal mesh, the dual mesh is not a cellular complex because some part of the boundary of a k-cell, $1 \le k \le 3$, in $\widetilde{M}$ is not in $\widetilde{M}$ if this cell touches the boundary $\partial\Omega$. For instance, for a primal vertex $v \in \partial\Omega$, only $\partial\tilde{c}(v) \cap \Omega$ consists of dual faces in $\widetilde{F}$; similarly, for a primal edge $e \subset \partial\Omega$, only $\partial\tilde{f}(e) \cap \Omega$ consists of dual edges in $\widetilde{E}$, and so on.

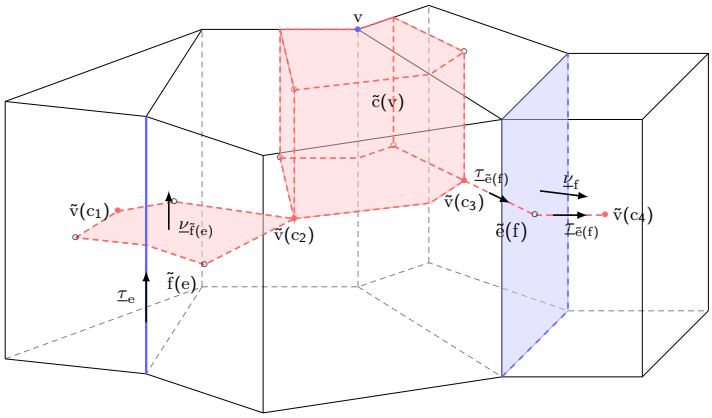

Figure 1: Examples of primal and dual mesh entities; note that in general dual edges are not straight segments (but consist of two straight segments) and dual faces are not planar (but consist of a finite number of triangles).

The analysis of CDO schemes requires some regularity assumptions on the underlying meshes. A rather general way to assert the regularity of polyhedral meshes is the following assumption, which we denote $(\mathbf{H}_M)$ in what follows: There exists a matching simplicial submesh that is shape-regular in the usual sense and that is a common refinement of both primal and dual meshes with each primal and dual cell containing a uniformly bounded number of subsimplices. Moreover, we assume for simplicity that primal faces are planar.

2.2 Discrete differential operators

The discrete differential operators on the primal mesh

$$\mathsf{GRAD} : \mathcal{V} \to \mathcal{E}, \qquad \mathsf{CURL} : \mathcal{E} \to \mathcal{F}, \qquad \mathsf{DIV} : \mathcal{F} \to \mathcal{C}, \tag{4a}$$

act such that, for all $\mathbf{p} = (\mathbf{p}_v)_{v\in V} \in \mathcal{V}$, $\mathbf{u} = (\mathbf{u}_e)_{e\in E} \in \mathcal{E}$ and $\boldsymbol{\phi} = (\boldsymbol{\phi}_f)_{f\in F} \in \mathcal{F}$,

$$\mathsf{GRAD}(\mathbf{p})|_e := \sum_{v\in V_e} \iota_{v,e}\mathbf{p}_v, \qquad \mathsf{CURL}(\mathbf{u})|_f := \sum_{e\in E_f} \iota_{e,f}\mathbf{u}_e, \qquad \mathsf{DIV}(\boldsymbol{\phi})|_c := \sum_{f\in F_c} \iota_{f,c}\boldsymbol{\phi}_f, \tag{4b}$$

where $V_e := \{v \in V \,|\, v \subset \partial e\}$ with $\iota_{v,e} = 1$ if $\underline{\tau}_e$ points towards v, $\iota_{v,e} = -1$ otherwise; $E_f := \{e \in E \,|\, e \subset \partial f\}$ with $\iota_{e,f} = 1$ if $\underline{\tau}_e$ shares the same orientation as that induced by $\underline{\nu}_f$ on ∂f, $\iota_{e,f} = -1$ otherwise; and $F_c := \{f \in F \,|\, f \subset \partial c\}$ with $\iota_{f,c} = 1$ if $\underline{\nu}_f$ points outward c, $\iota_{f,c} = -1$ otherwise. Algebraically, the discrete differential operators are represented by an incidence matrix (with entries in $\{0, \pm 1\}$). This reflects the topological or metric-free nature of these operators, which is a feature shared by many mimetic schemes; see e.g. [12, 18, 44, 9, 22, 30, 40]. The discrete differential operators commute with

the de Rham maps,

$$\mathsf{R}_{\mathcal{E}}(\underline{\mathrm{grad}}) = \mathsf{GRAD}(\mathsf{R}_{\mathcal{V}}), \quad \mathsf{R}_{\mathcal{F}}(\underline{\mathrm{curl}}) = \mathsf{CURL}(\mathsf{R}_{\mathcal{E}}), \quad \mathsf{R}_{\mathcal{C}}(\mathrm{div}) = \mathsf{DIV}(\mathsf{R}_{\mathcal{F}}), \tag{5}$$

they produce a cochain complex,

$$\mathsf{CURL}(\mathsf{GRAD}) = 0_{\mathcal{F}}, \quad \mathsf{DIV}(\mathsf{CURL}) = 0_{\mathcal{C}}, \tag{6}$$

and, under assumption ($\mathbf{H_\Omega}$), they generate an exact sequence,

$$\mathrm{Im}\,\mathsf{GRAD} = \mathrm{Ker}\,\mathsf{CURL}, \quad \mathrm{Im}\,\mathsf{CURL} = \mathrm{Ker}\,\mathsf{DIV}, \tag{7}$$

where Im is the range of an operator and Ker the kernel.

The discrete differential operators on the dual mesh

$$\widetilde{\mathsf{GRAD}} : \widetilde{\mathcal{V}} \to \widetilde{\mathcal{E}}, \qquad \widetilde{\mathsf{CURL}} : \widetilde{\mathcal{E}} \to \widetilde{\mathcal{F}}, \qquad \widetilde{\mathsf{DIV}} : \widetilde{\mathcal{F}} \to \widetilde{\mathcal{C}}, \tag{8}$$

are defined similarly to (4b). For instance, $\widetilde{\mathsf{GRAD}}(\mathbf{p})|_{\tilde{\mathrm{e}}} := \sum_{\tilde{\mathrm{v}} \in \widetilde{\mathrm{V}}_{\tilde{\mathrm{e}}}} \iota_{\tilde{\mathrm{v}},\tilde{\mathrm{e}}} \mathbf{p}_{\tilde{\mathrm{v}}}$ for all $\mathbf{p} = (\mathbf{p}_{\tilde{\mathrm{v}}})_{\tilde{\mathrm{v}} \in \widetilde{\mathrm{V}}} \in \widetilde{\mathcal{V}}$, and so on. Notice that the sets $\widetilde{\mathrm{V}}_{\tilde{\mathrm{e}}}$, $\widetilde{\mathrm{E}}_{\tilde{\mathrm{f}}}$, and $\widetilde{\mathrm{F}}_{\tilde{\mathrm{c}}}$ do not contain geometric entities located at the boundary $\partial\Omega$; for instance, if the dual edge $\tilde{\mathrm{e}}$ is associated with a primal face $\mathrm{f} \subset \partial\Omega$, then the set $\widetilde{\mathrm{V}}_{\tilde{\mathrm{e}}}$ contains only one dual vertex (the extremity of $\tilde{\mathrm{e}}$ located in Ω). The discrete differential operators on the dual mesh commute with the de Rham maps on all interior dual mesh entities,

$$\mathsf{R}_{\widetilde{\mathcal{E}}}(\underline{\mathrm{grad}})|_{\tilde{\mathrm{e}}} = \widetilde{\mathsf{GRAD}}(\mathsf{R}_{\widetilde{\mathcal{V}}})|_{\tilde{\mathrm{e}}}, \quad \mathsf{R}_{\widetilde{\mathcal{F}}}(\underline{\mathrm{curl}})|_{\tilde{\mathrm{f}}} = \widetilde{\mathsf{CURL}}(\mathsf{R}_{\widetilde{\mathcal{E}}})|_{\tilde{\mathrm{f}}}, \quad \mathsf{R}_{\widetilde{\mathcal{C}}}(\mathrm{div})|_{\tilde{\mathrm{c}}} = \widetilde{\mathsf{DIV}}(\mathsf{R}_{\widetilde{\mathcal{F}}})|_{\tilde{\mathrm{c}}}, \tag{9}$$

for all $\tilde{\mathrm{e}}$, $\tilde{\mathrm{f}}$, and $\tilde{\mathrm{c}}$ which do not intersect the boundary $\partial\Omega$. Moreover, these operators produce a cochain complex,

$$\widetilde{\mathsf{CURL}}(\widetilde{\mathsf{GRAD}}) = 0_{\widetilde{\mathcal{F}}}, \quad \widetilde{\mathsf{DIV}}(\widetilde{\mathsf{CURL}}) = 0_{\widetilde{\mathcal{C}}}. \tag{10}$$

and, under assumption ($\mathbf{H_\Omega}$), they generate an exact sequence,

$$\mathrm{Im}\,\widetilde{\mathsf{GRAD}} = \mathrm{Ker}\,\widetilde{\mathsf{CURL}}, \quad \mathrm{Im}\,\widetilde{\mathsf{CURL}} = \mathrm{Ker}\,\widetilde{\mathsf{DIV}}. \tag{11}$$

The last important property is an adjunction between discrete differential operators on the primal and dual meshes. We define global duality products as follows:

$$\big[\!\big[\mathbf{p}, \mathbf{s}\big]\!\big]_{\mathcal{V}\widetilde{\mathcal{C}}} := \sum_{\mathrm{v} \in \mathrm{V}} \mathbf{p}_{\mathrm{v}} \mathbf{s}_{\tilde{\mathrm{c}}(\mathrm{v})}, \qquad \big[\!\big[\mathbf{u}, \boldsymbol{\phi}\big]\!\big]_{\mathcal{E}\widetilde{\mathcal{F}}} := \sum_{\mathrm{e} \in \mathrm{E}} \mathbf{u}_{\mathrm{e}} \boldsymbol{\phi}_{\tilde{\mathrm{f}}(\mathrm{e})}, \tag{12a}$$

$$\big[\!\big[\mathbf{s}, \mathbf{p}\big]\!\big]_{\mathcal{C}\widetilde{\mathcal{V}}} := \sum_{\mathrm{c} \in \mathrm{C}} \mathbf{s}_{\mathrm{c}} \mathbf{p}_{\tilde{\mathrm{v}}(\mathrm{c})}, \qquad \big[\!\big[\boldsymbol{\phi}, \mathbf{u}\big]\!\big]_{\mathcal{F}\widetilde{\mathcal{E}}} := \sum_{\mathrm{f} \in \mathrm{F}} \boldsymbol{\phi}_{\mathrm{f}} \mathbf{u}_{\tilde{\mathrm{e}}(\mathrm{f})}, \tag{12b}$$

for all $(\mathbf{p}, \mathbf{s}) \in \mathcal{V} \times \widetilde{\mathcal{C}}$ and $(\mathbf{u}, \boldsymbol{\phi}) \in \mathcal{E} \times \widetilde{\mathcal{F}}$ in (12a) and for all $(\mathbf{s}, \mathbf{p}) \in \mathcal{C} \times \widetilde{\mathcal{V}}$ and $(\boldsymbol{\phi}, \mathbf{u}) \in \mathcal{F} \times \widetilde{\mathcal{E}}$ in (12b). Then, the following identities hold:

$$\forall (\mathbf{p}, \boldsymbol{\phi}) \in \mathcal{V} \times \widetilde{\mathcal{F}}, \qquad \big[\!\big[\mathsf{GRAD}(\mathbf{p}), \boldsymbol{\phi}\big]\!\big]_{\mathcal{E}\widetilde{\mathcal{F}}} = -\big[\!\big[\mathbf{p}, \widetilde{\mathsf{DIV}}(\boldsymbol{\phi})\big]\!\big]_{\mathcal{V}\widetilde{\mathcal{C}}}, \tag{13a}$$

$$\forall (\mathbf{u}, \boldsymbol{\omega}) \in \mathcal{E} \times \widetilde{\mathcal{E}}, \qquad \big[\!\big[\mathsf{CURL}(\mathbf{u}), \mathbf{v}\big]\!\big]_{\mathcal{F}\widetilde{\mathcal{E}}} = \big[\!\big[\mathbf{u}, \widetilde{\mathsf{CURL}}(\mathbf{v})\big]\!\big]_{\mathcal{E}\widetilde{\mathcal{F}}}, \tag{13b}$$

$$\forall (\boldsymbol{\phi}, \mathbf{p}) \in \mathcal{F} \times \widetilde{\mathcal{V}}, \qquad \big[\!\big[\mathsf{DIV}(\boldsymbol{\phi}), \mathbf{p}\big]\!\big]_{\mathcal{C}\widetilde{\mathcal{V}}} = -\big[\!\big[\boldsymbol{\phi}, \widetilde{\mathsf{GRAD}}(\mathbf{p})\big]\!\big]_{\mathcal{F}\widetilde{\mathcal{E}}}. \tag{13c}$$

Algebraically, the matrix representing a discrete differential operator on the dual mesh is the transpose of that of the corresponding operator on the primal mesh.

2.3 Discrete Hodge operators

In the CDO framework, the crucial point is the design of the discrete Hodge operator. This operator is related to the discretization of a constitutive relation, and in contrast to discrete differential operators, its design is not uniquely defined. The discrete Hodge operator maps DoFs attached to primal mesh entities to DoFs attached to the corresponding dual mesh entities in one-to-one pairing, and is algebraically represented by a (square) symmetric positive definite (SPD) matrix. A generic discrete Hodge operator is denoted $\mathsf{H}_\alpha^{\mathcal{X}\widetilde{\mathcal{Y}}}$ with ${}_{\mathcal{X}}\widetilde{\mathcal{Y}} \in \{{}_{\mathcal{V}}\widetilde{\mathcal{C}}, {}_{\mathcal{E}}\widetilde{\mathcal{F}}, {}_{\mathcal{F}}\widetilde{\mathcal{E}}, {}_{\mathcal{C}}\widetilde{\mathcal{V}}\}$ and where α refers to the material property involved in the constitutive relation. The set of primal (resp., dual) mesh entities associated with $\mathcal{X}$ (resp., $\widetilde{\mathcal{Y}}$) is denoted X (resp., $\widetilde{\mathrm{Y}}$).

In the context of the Stokes equations, the two most salient discrete Hodge operators are $\mathsf{H}_\alpha^{\mathcal{E}\widetilde{\mathcal{F}}}$ and $\mathsf{H}_\alpha^{\mathcal{F}\widetilde{\mathcal{E}}}$, so that we focus on the case where ${}_{\mathcal{X}}\widetilde{\mathcal{Y}} \in \{{}_{\mathcal{E}}\widetilde{\mathcal{F}}, {}_{\mathcal{F}}\widetilde{\mathcal{E}}\}$. These operators are assembled from local discrete Hodge operators attached to primal cells. Let $\mathrm{c} \in \mathrm{C}$. We introduce the local subsets

$$\mathrm{X}_\mathrm{c} := \{\mathrm{x} \in \mathrm{X} \,|\, \mathrm{x} \subseteq \partial\mathrm{c}\}, \qquad \widetilde{\mathrm{Y}}_\mathrm{c} := \{\tilde{\mathrm{y}}_\mathrm{c}(\mathrm{x}) := \tilde{\mathrm{y}}(\mathrm{x}) \cap \mathrm{c},\, \mathrm{x} \in \mathrm{X}_\mathrm{c}\}. \tag{14}$$

In particular, we need the local subsets $\mathrm{E}_\mathrm{c} := \{\mathrm{e} \in \mathrm{E} \,|\, \mathrm{e} \subset \partial\mathrm{c}\}$ and $\widetilde{\mathrm{F}}_\mathrm{c} := \{\tilde{\mathrm{f}}_\mathrm{c}(\mathrm{e}) := \tilde{\mathrm{f}}(\mathrm{e}) \cap \mathrm{c} \,|\, \mathrm{e} \in \mathrm{E}_\mathrm{c}\}$, and $\mathrm{F}_\mathrm{c} := \{\mathrm{f} \in \mathrm{F} \,|\, \mathrm{f} \subset \partial\mathrm{c}\}$ and $\widetilde{\mathrm{E}}_\mathrm{c} := \{\tilde{\mathrm{e}}_\mathrm{c}(\mathrm{f}) := \tilde{\mathrm{e}}(\mathrm{f}) \cap \mathrm{c} \,|\, \mathrm{f} \in \mathrm{F}_\mathrm{c}\}$. The local de Rham maps $\mathsf{R}_{\mathcal{X}_\mathrm{c}}$ mapping onto the space of local primal DoFs $\mathcal{X}_\mathrm{c}$ are defined as in (3), while the local de Rham maps $\mathsf{R}_{\widetilde{\mathcal{Y}}_\mathrm{c}}$ mapping onto the space of local dual DoFs $\widetilde{\mathcal{Y}}_\mathrm{c}$ are defined by restricting the domain of integration to c; for instance,

$$(\mathsf{R}_{\widetilde{\mathcal{E}}_\mathrm{c}}(\underline{u}))_{\tilde{\mathrm{e}}_\mathrm{c}(\mathrm{f})} := \int_{\tilde{\mathrm{e}}_\mathrm{c}(\mathrm{f})} \underline{u} \cdot \underline{\tau}_{\tilde{\mathrm{e}}_\mathrm{c}(\mathrm{f})}, \qquad (\mathsf{R}_{\widetilde{\mathcal{F}}_\mathrm{c}}(\underline{\phi}))_{\tilde{\mathrm{f}}_\mathrm{c}(\mathrm{e})} := \int_{\tilde{\mathrm{f}}_\mathrm{c}(\mathrm{e})} \underline{\phi} \cdot \underline{\nu}_{\tilde{\mathrm{f}}_\mathrm{c}(\mathrm{e})}, \tag{15}$$

where $\underline{\tau}_{\tilde{\mathrm{e}}_\mathrm{c}(\mathrm{f})}$ (resp., $\underline{\nu}_{\tilde{\mathrm{f}}_\mathrm{c}(\mathrm{e})}$) is consistently oriented by $\underline{\nu}_\mathrm{f}$ (resp., $\underline{\tau}_\mathrm{e}$). Then, the assembly of $\mathsf{H}_\alpha^{\mathcal{X}\widetilde{\mathcal{Y}}}$ can be written as

$$\mathsf{H}_\alpha^{\mathcal{X}\widetilde{\mathcal{Y}}} = \sum_{\mathrm{c}\in\mathrm{C}} \mathsf{P}_{\mathcal{X},\mathrm{c}}^* \cdot \mathsf{H}_\alpha^{\mathcal{X}_\mathrm{c}\widetilde{\mathcal{Y}}_\mathrm{c}} \cdot \mathsf{P}_{\mathcal{X},\mathrm{c}}, \tag{16}$$

where $\mathsf{P}_{\mathcal{X},\mathrm{c}} : \mathcal{X} \to \mathcal{X}_\mathrm{c}$ is the (full-rank) map from global to local spaces of DoFs, $\mathsf{P}_{\mathcal{X},\mathrm{c}}^*$ the adjoint map, and $\mathsf{H}_\alpha^{\mathcal{X}_\mathrm{c}\widetilde{\mathcal{Y}}_\mathrm{c}} : \mathcal{X}_\mathrm{c} \to \widetilde{\mathcal{Y}}_\mathrm{c}$ the local discrete Hodge operator attached to the primal cell c. Observe that $\mathsf{H}_\alpha^{\mathcal{X}\widetilde{\mathcal{Y}}}$ is algebraically represented by a (large) sparse SPD matrix of order $\#\mathrm{X} = \#\widetilde{\mathrm{Y}}$, while $\mathsf{H}_\alpha^{\mathcal{X}_\mathrm{c}\widetilde{\mathcal{Y}}_\mathrm{c}}$ is algebraically represented by a (small) dense SPD matrix of order $\#\mathrm{X}_\mathrm{c} = \#\widetilde{\mathrm{Y}}_\mathrm{c}$.

The local discrete Hodge operators $\mathsf{H}_\alpha^{\mathcal{X}_\mathrm{c}\widetilde{\mathcal{Y}}_\mathrm{c}}$ must fulfil, for all $\mathrm{c} \in \mathrm{C}$, two key properties: stability and $\mathbb{P}_0$-consistency; see [11]. To state these properties, we introduce some notation. Similarly to (12), we define local duality products as $[\![\mathbf{a}, \mathbf{b}]\!]_{\mathcal{X}_\mathrm{c}\widetilde{\mathcal{Y}}_\mathrm{c}} := \sum_{\mathrm{x}\in\mathrm{X}_\mathrm{c}} \mathbf{a}_\mathrm{x} \mathbf{b}_{\tilde{\mathrm{y}}_\mathrm{c}(\mathrm{x})}$ for all $(\mathbf{a}, \mathbf{b}) \in \mathcal{X}_\mathrm{c} \times \widetilde{\mathcal{Y}}_\mathrm{c}$. We introduce the local mesh-dependent norm

$$\forall \mathbf{a} \in \mathcal{X}_\mathrm{c}, \qquad |\!|\!|\mathbf{a}|\!|\!|_{2,\mathcal{X}_\mathrm{c}}^2 := \sum_{\mathrm{x}\in\mathrm{X}_\mathrm{c}} |\mathfrak{p}_{\mathrm{x},\mathrm{c}}| \left(\frac{\mathbf{a}_\mathrm{x}}{|\mathrm{x}|}\right)^2, \tag{17}$$

where $\mathfrak{p}_{\mathrm{x},\mathrm{c}}$ denotes a subvolume of c attached to the primal mesh entity x. There are several possible definitions for these subvolumes; an example is presented in Figure 2 for vertices, edges, and faces using a barycentric subdivision of an hexahedral cell. Observe that owing to mesh regularity, see ($\mathbf{H}_\mathrm{M}$), the measure of $\mathfrak{p}_{\mathrm{x},\mathrm{c}}$ is uniformly equivalent to h_c^3, where h_c denotes the diameter of c. Then, the stability and $\mathbb{P}_0$-consistency properties of the local discrete Hodge operators assert that, for all $\mathrm{c} \in \mathrm{C}$,

($\mathbf{A}1$) [Stability] There exists $\eta_\alpha > 0$ such that

$$\forall \mathbf{a} \in \mathcal{X}_\mathrm{c}, \quad \eta_\alpha |\!|\!|\mathbf{a}|\!|\!|_{2,\mathcal{X}_\mathrm{c}}^2 \le [\![\mathbf{a}, \mathsf{H}_\alpha^{\mathcal{X}_\mathrm{c}\widetilde{\mathcal{Y}}_\mathrm{c}}(\mathbf{a})]\!]_{\mathcal{X}_\mathrm{c}\widetilde{\mathcal{Y}}_\mathrm{c}} \le \eta_\alpha^{-1} |\!|\!|\mathbf{a}|\!|\!|_{2,\mathcal{X}_\mathrm{c}}^2. \tag{18}$$

($\mathbf{A}2$) [$\mathbb{P}_0$-consistency] The local commuting operator $\lfloor \alpha, {}_{\mathcal{X}_\mathrm{c}}\widetilde{\mathcal{Y}}_\mathrm{c} \rceil(\bullet) := \mathsf{H}_\alpha^{\mathcal{X}_\mathrm{c}\widetilde{\mathcal{Y}}_\mathrm{c}} \cdot \mathsf{R}_{\mathcal{X}_\mathrm{c}}(\bullet) - \mathsf{R}_{\widetilde{\mathcal{Y}}_\mathrm{c}}(\alpha\bullet)$ satisfies $\lfloor \alpha, {}_{\mathcal{X}_\mathrm{c}}\widetilde{\mathcal{Y}}_\mathrm{c} \rceil(\underline{C}) = 0$ for all $\underline{C}$ constant in c.

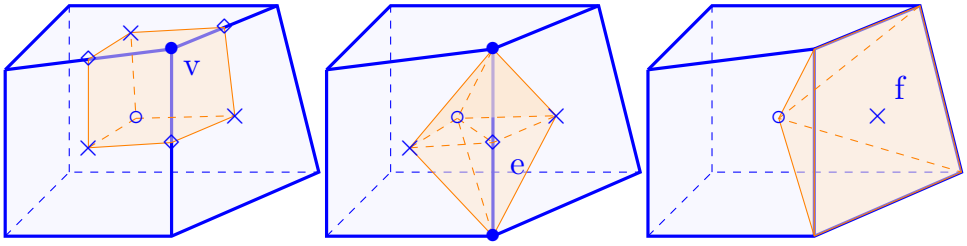

Figure 2: Hexahedral mesh cell c. Left: Example for $\mathfrak{p}_{\mathrm{v},\mathrm{c}}$; Middle: Example for $\mathfrak{p}_{\mathrm{e},\mathrm{c}}$; Right: Example for $\mathfrak{p}_{\mathrm{f},\mathrm{c}}$.

These two properties share the same spirit as those introduced for MFD schemes by [14, 16]. One way to design local discrete Hodge operators matching these two properties is to define them as local mass matrices built from reconstruction functions satisfying suitable properties inspired from the Discrete Geometric Approach of [19]; see [11].

2.4 Discrete functional analysis

We introduce global mesh-dependent norms by summing cellwise the local mesh-dependent norms defined by (17), i.e., $\|\mathbf{a}\|_{2,\mathcal{X}}^2 := \sum_{\mathrm{c}\in\mathrm{C}}\|\mathsf{P}_{\mathcal{X}_\mathrm{c}}(\mathbf{a})\|_{2,\mathcal{X}_\mathrm{c}}^2$. Summing cellwise (**A**1) and using (16), we infer that

$$\forall \mathbf{a}\in\mathcal{X},\qquad \eta_\alpha\|\mathbf{a}\|_{2,\mathcal{X}}^2 \le \|\mathbf{a}\|_{\alpha,\mathcal{X}}^2 := \left[\!\left[\mathbf{a},\mathsf{H}_\alpha^{\mathcal{X}\tilde{\mathcal{Y}}}(\mathbf{a})\right]\!\right]_{\mathcal{X}\tilde{\mathcal{Y}}} \le \eta_\alpha^{-1}\|\mathbf{a}\|_{2,\mathcal{X}}^2. \tag{19}$$

Whenever the context is unambiguous, we write $\|\mathbf{a}\|_\alpha$ instead of $\|\mathbf{a}\|_{\alpha,\mathcal{X}}$.

The following two discrete Poincaré inequalities are important tools for the analysis of CDO schemes applied to the Stokes equations. We postpone their proof to Appendix A. The discrete Hodge operator $\mathsf{H}_1^{\mathcal{V}\tilde{\mathcal{C}}}$ in Lemma 2.1 is diagonal with entries equal to $|\tilde{\mathrm{c}}(\mathrm{v})|$, while $\mathbf{1}\in\mathcal{V}$ has entries equal to 1. The discrete Hodge operator $\mathsf{H}_\alpha^{\mathcal{E}\tilde{\mathcal{F}}}$ in Lemma 2.2 only needs to satisfy the stability property (**A**1).

Lemma 2.1 (Discrete Poincaré–Wirtinger inequality)**.** *Assume (*$\mathbf{H}_\mathrm{M}$*). Then, there exists* $C_\mathrm{P}^{(0)}$ *(independent of the mesh size, but dependent on mesh regularity) such that, for all* $\mathbf{p}\in\mathcal{V}$ *verifying* $\left[\!\left[\mathbf{p},\mathsf{H}_1^{\mathcal{V}\tilde{\mathcal{C}}}(\mathbf{1})\right]\!\right]_{\mathcal{V}\tilde{\mathcal{C}}}=0$*, the following inequality holds:*

$$\|\mathbf{p}\|_{2,\mathcal{V}} \le C_\mathrm{P}^{(0)}\|\mathsf{GRAD}(\mathbf{p})\|_{2,\mathcal{E}}. \tag{20}$$

Lemma 2.2 (Discrete Poincaré inequality for the curl)**.** *Assume (*$\mathbf{H}_\mathrm{M}$*) and (*$\mathbf{H}_\Omega$*). Let* $\mathsf{H}_\alpha^{\mathcal{E}\tilde{\mathcal{F}}}$ *satisfy (***A**1*). Then, there exists* $C_\mathrm{P}^{(1)}$ *(independent of the mesh size, but dependent on mesh regularity and the stability constant* η_α*) such that, for all* $\mathbf{u}\in\mathcal{E}$ *such that* $\left[\!\left[\mathbf{u},\mathsf{H}_\alpha^{\mathcal{E}\tilde{\mathcal{F}}}(\mathbf{v})\right]\!\right]_{\mathcal{E}\tilde{\mathcal{F}}}=0$ *for all* $\mathbf{v}\in\mathrm{Ker}\,\mathsf{CURL}$*, the following inequality holds:*

$$\|\mathbf{u}\|_{2,\mathcal{E}} \le C_\mathrm{P}^{(1)}\|\mathsf{CURL}(\mathbf{u})\|_{2,\mathcal{F}}. \tag{21}$$

2.5 Bound on consistency error

In CDO schemes, the discrete errors are bounded only by the consistency error introduced by the lack of commuting property of the discrete Hodge operators with the de Rham maps; see [12], [31], [20], and [11]. Recalling (**A**2), the global commuting operators are defined as follows:

$$\lfloor\alpha,\,{}^{\mathcal{X}}\tilde{\mathcal{Y}}\rceil(\bullet) := \mathsf{H}_\alpha^{\mathcal{X}\tilde{\mathcal{Y}}}\cdot\mathsf{R}_{\mathcal{X}}(\bullet) - \mathsf{R}_{\tilde{\mathcal{Y}}}(\alpha\bullet). \tag{22}$$

We define the discrete norm such that $\|\mathbf{b}\|_{\alpha^{-1},\tilde{\mathcal{Y}}}^2 := \left[(\mathsf{H}_\alpha^{\mathcal{X}\tilde{\mathcal{Y}}})^{-1}(\mathbf{b}),\mathbf{b}\right]_{\mathcal{X}\tilde{\mathcal{Y}}}$ for all $\mathbf{b}\in\tilde{\mathcal{Y}}$. Whenever the context is unambiguous, we write $\|\mathbf{b}\|_{\alpha^{-1}}$ instead of $\|\mathbf{b}\|_{\alpha^{-1},\tilde{\mathcal{Y}}}$.

In what follows, we abbreviate $A \lesssim B$ the inequality $A \le cB$ with positive constant c whose value can change at each occurrence and is independent of any mesh size (but can depend on the mesh regularity and the stability constants of the discrete Hodge operators). Let $H^1(\mathrm{C})$ denote the broken Sobolev space H^1 on the primal mesh. Let $h_\mathrm{M} := \max_{\mathrm{c}\in\mathrm{C}} h_c$ denote the maximal mesh size. We now derive a first-order estimate on the consistency error for smooth enough vector fields.

Lemma 2.3 (Error bound for smooth fields)**.** *Assume (*$\mathbf{H}_\mathrm{M}$*). Let* $\underline{b} \in H^1(\mathrm{C})^3$ *be such that* $\underline{\mathrm{curl}}(\underline{b}) \in L^4(\Omega)^3$*. Let* $\mathsf{H}_\alpha^{\scriptscriptstyle\mathsf{x}\tilde{\mathsf{y}}}$ *satisfy (*$\mathbf{A}1$*) and (*$\mathbf{A}2$*) with* $\mathsf{x}\tilde{\mathsf{y}} = \varepsilon\tilde{\mathsf{f}}$ *or* $\mathsf{f}\tilde{\mathsf{e}}$*. Then, the following inequality holds:*

$$\|\!|\lfloor\alpha,\, \mathsf{x}\tilde{\mathsf{y}}\rceil(\underline{b})|\!\|^2_{\alpha^{-1},\widetilde{\mathcal{Y}}} \lesssim h_\mathrm{M}^2 \left(\|\underline{b}\|^2_{H^1(\mathrm{C})^3} + \|\underline{\mathrm{curl}}\,\underline{b}\|^2_{L^4(\Omega)^3}\right). \tag{23}$$

Proof. We preliminarily observe that the smoothness assumption on $\underline{b}$ entails that this vector field is in the domain of the de Rham maps $\mathsf{R}_\mathcal{E}$, $\mathsf{R}_\mathcal{F}$, $\mathsf{R}_{\widetilde{\mathcal{E}}}$ and $\mathsf{R}_{\widetilde{\mathcal{F}}}$; see in particular [36]. We only prove (23) for $\mathsf{x}\tilde{\mathsf{y}} = \varepsilon\tilde{\mathsf{f}}$, the proof for $\mathsf{x}\tilde{\mathsf{y}} = \mathsf{f}\tilde{\mathsf{e}}$ being similar. The proof follows the same lines as [11, Theorem 3.3]. Using the algebraic result of [20, Theorem 9] yields $\|\!|\lfloor\alpha,\, \varepsilon\tilde{\mathsf{f}}\rceil(\underline{b})|\!\|^2_{\alpha^{-1},\widetilde{\mathcal{F}}} \le \sum_{\mathrm{c}\in\mathrm{C}}(T_\mathrm{c})^2$ where $(T_\mathrm{c})^2 := \|\!|\lfloor\alpha,\, \varepsilon_\mathrm{c}\tilde{\mathcal{F}}_\mathrm{c}\rceil(\underline{b})|\!\|^2_{\alpha^{-1},\widetilde{\mathcal{F}}_\mathrm{c}}$ with $\|\mathbf{b}\|^2_{\alpha^{-1},\widetilde{\mathcal{F}}_\mathrm{c}} := \left[(\mathsf{H}_\alpha^{\varepsilon_\mathrm{c}\tilde{\mathcal{F}}_\mathrm{c}})^{-1}(\mathbf{b}), \mathbf{b}\right]_{\varepsilon_\mathrm{c}\tilde{\mathcal{F}}_\mathrm{c}}$ for all $\mathbf{b} \in \widetilde{\mathcal{F}}_\mathrm{c}$. Then, owing to $(\mathbf{A}1)$, $(\mathbf{A}2)$, the triangle inequality, and $(\mathbf{H}_\mathrm{M})$, we infer that

$$(T_\mathrm{c})^2 = \|\!|\lfloor\alpha,\, \varepsilon_\mathrm{c}\tilde{\mathcal{F}}_\mathrm{c}\rceil((\underline{b}-\underline{B})|_\mathrm{c})|\!\|^2_{\alpha^{-1},\widetilde{\mathcal{F}}_\mathrm{c}} \lesssim h_\mathrm{c} \sum_{\mathrm{e}\in\mathrm{E}_\mathrm{c}} |T_\mathrm{e}|^2 + h_\mathrm{c}^{-1} \sum_{\mathrm{e}\in\mathrm{E}} |T_{\tilde{\mathrm{f}}_\mathrm{c}(\mathrm{e})}|^2,$$

where $T_{\tilde{\mathrm{f}}_\mathrm{c}(\mathrm{e})} := \int_{\tilde{\mathrm{f}}_\mathrm{c}(\mathrm{e})} (\underline{b}-\underline{B})\cdot\underline{\nu}_{\tilde{\mathrm{f}}_\mathrm{c}(\mathrm{e})}$, $T_\mathrm{e} := \int_\mathrm{e} (\underline{b}-\underline{B})\cdot\underline{\tau}_\mathrm{e}$, and $\underline{B}$ is the piecewise constant approximation of $\underline{b}$ on the primal mesh. Using mesh regularity and approximation results, we finally obtain that $|T_{\tilde{\mathrm{f}}_\mathrm{c}(\mathrm{e})}|^2 \lesssim h_\mathrm{c}^3 \|\underline{b}\|^2_{H^1(\mathrm{c})^3}$ and $|T_\mathrm{e}|^2 \lesssim h_\mathrm{c} \left(\|\underline{b}\|^2_{H^1(\mathrm{c})^3} + \|\underline{\mathrm{curl}}\,\underline{b}\|^2_{L^4(\mathrm{c})^3}\right)$; see [2, Lemma 4.7] applied with $p = 4$. □

3 Vertex-Based Pressure Schemes

3.1 Discrete systems

In vertex-based pressure schemes, the starting formulation is the 2-field curl formulation (1). Although the mass density ρ and the viscosity μ are constant, we rewrite (1) using these material properties so as to identify where a discrete Hodge operator should be used. We obtain

$$\begin{cases} \underline{\mathrm{curl}}(\mu\,\underline{\mathrm{curl}}(\underline{u})) + \rho\,\underline{\mathrm{grad}}(p^*) = \rho\underline{f}^*, & \text{in } \Omega, \\ \mathrm{div}(\rho\underline{u}) = 0, & \text{in } \Omega, \end{cases} \tag{24}$$

where we have introduced the pressure potential $p^* := \rho^{-1}p$ and the external load density $\underline{f}^* := \rho^{-1}\underline{f}$. We focus on natural BCs for (24), which are given by

$$\rho\underline{u}\cdot\underline{\nu}_{\partial\Omega} = u_\nu^{\mathrm{bc}}, \quad \mu\underline{\omega}\times\underline{\nu}_{\partial\Omega} = \underline{\omega}_\tau^{\mathrm{bc}}, \qquad \text{on } \partial\Omega, \tag{25}$$

with data u_ν^{bc} and $\underline{\omega}_\tau^{\mathrm{bc}}$; for essential BCs, see Remark 3.1. In what follows, we also consider the mass flux $\underline{\phi} := \rho\underline{u}$, the vorticity $\underline{\omega} = \underline{\mathrm{curl}}(\underline{u})$, and the auxiliary field $\underline{\omega}^* := \mu\underline{\omega}$ to which we loosely refer as viscous stress circulation. With these quantities, (24) can be rewritten as $\underline{\mathrm{curl}}(\underline{\omega}^*) + \rho\,\underline{\mathrm{grad}}(p^*) = \rho\underline{f}^*$ and $\mathrm{div}(\underline{\phi}) = 0$ in Ω.

In vertex-based pressure schemes, the two unknowns are the pressure potential p^* and the velocity $\underline{u}$. The DoFs of the pressure potential, denoted $\mathbf{p}^*$, are located at primal vertices. The DoFs of the velocity, denoted $\mathbf{u}$, are located at primal edges. The velocity field is therefore seen as a circulation. The vorticity DoFs, which are located at primal faces, are directly obtained from the velocity DoFs by setting $\boldsymbol{\omega} := \mathsf{CURL}(\mathbf{u})$. The translational invariance of the discrete pressure potential is fixed by the condition

$$\left[\!\left[\mathbf{p}^*, \mathsf{H}_1^{\nu\tilde{c}}(\mathbf{1})\right]\!\right]_{\nu\tilde{c}} = 0, \tag{26}$$

where $\mathsf{H}_1^{\mathcal{V}\widetilde{\mathcal{C}}}$ and $\mathbf{1}$ are defined before Lemma 2.1, so that (26) can be rewritten as $\sum_{\mathrm{v}\in\mathrm{V}}|\tilde{\mathrm{c}}(\mathrm{v})|\mathbf{p}^*_{\mathrm{v}} = 0$, which is the discrete counterpart of the zero mean-value condition on the pressure.

There are two discrete Hodge operators, one related to the mass density ρ and the other to the viscosity μ. The discrete Hodge operator $\mathsf{H}_\rho^{\mathcal{E}\widetilde{\mathcal{F}}}$ allows us to define the discrete mass flux $\boldsymbol{\phi} := \mathsf{H}_\rho^{\mathcal{E}\widetilde{\mathcal{F}}}(\mathbf{u})$ located at dual faces (compare with $\underline{\phi} = \rho\underline{u}$), and the discrete Hodge operator $\mathsf{H}_\mu^{\mathcal{F}\widetilde{\mathcal{E}}}$ the discrete viscous stress circulation $\boldsymbol{\omega}^* := \mathsf{H}_\mu^{\mathcal{F}\widetilde{\mathcal{E}}}(\boldsymbol{\omega})$ located at dual edges (compare with $\underline{\omega}^* := \mu\underline{\omega}$). Both discrete Hodge operators are assumed to satisfy the stability and $\mathbb{P}_0$-consistency properties (**A**1) and (**A**2). In what follows, we consider the following discrete norms:

$$\|\mathbf{u}\|_\rho^2 := \left[\!\left[\mathbf{u}, \mathsf{H}_\rho^{\mathcal{E}\widetilde{\mathcal{F}}}(\mathbf{u})\right]\!\right]_{\mathcal{E}\widetilde{\mathcal{F}}}, \qquad \|\boldsymbol{\phi}\|_{\rho^{-1}}^2 := \left[\!\left[(\mathsf{H}_\rho^{\mathcal{E}\widetilde{\mathcal{F}}})^{-1}(\boldsymbol{\phi}), \boldsymbol{\phi}\right]\!\right]_{\mathcal{E}\widetilde{\mathcal{F}}}, \tag{27a}$$

$$\|\boldsymbol{\omega}\|_\mu^2 := \left[\!\left[\boldsymbol{\omega}, \mathsf{H}_\mu^{\mathcal{F}\widetilde{\mathcal{E}}}(\boldsymbol{\omega})\right]\!\right]_{\mathcal{F}\widetilde{\mathcal{E}}}, \qquad \|\boldsymbol{\omega}^*\|_{\mu^{-1}}^2 := \left[\!\left[(\mathsf{H}_\mu^{\mathcal{F}\widetilde{\mathcal{E}}})^{-1}(\boldsymbol{\omega}^*), \boldsymbol{\omega}^*\right]\!\right]_{\mathcal{F}\widetilde{\mathcal{E}}}, \tag{27b}$$

for all $\mathbf{u} \in \mathcal{E}$, $\boldsymbol{\phi} \in \widetilde{\mathcal{F}}$, $\boldsymbol{\omega} \in \mathcal{F}$, and $\boldsymbol{\omega}^* \in \widetilde{\mathcal{E}}$. Owing to the Cauchy–Schwarz inequality, we infer that

$$\left[\!\left[\mathbf{u}, \boldsymbol{\phi}\right]\!\right]_{\mathcal{E}\widetilde{\mathcal{F}}} \le \|\mathbf{u}\|_\rho \, \|\boldsymbol{\phi}\|_{\rho^{-1}}, \qquad \left[\!\left[\boldsymbol{\omega}, \boldsymbol{\omega}^*\right]\!\right]_{\mathcal{F}\widetilde{\mathcal{E}}} \le \|\boldsymbol{\omega}\|_\mu \, \|\boldsymbol{\omega}^*\|_{\mu^{-1}}. \tag{28}$$

We introduce the following operators:

$$\begin{aligned} &\mathsf{A}^{\mathsf{vb}} : \mathcal{E} \to \widetilde{\mathcal{F}}, && \mathsf{B} : \mathcal{E} \to \widetilde{\mathcal{C}}, && \mathsf{B}^{\mathrm{T}} : \mathcal{V} \to \widetilde{\mathcal{F}}, \\ &\mathsf{A}^{\mathsf{vb}} := \widetilde{\mathsf{CURL}} \cdot \mathsf{H}_\mu^{\mathcal{F}\widetilde{\mathcal{E}}} \cdot \mathsf{CURL}, && \mathsf{B} := -\widetilde{\mathsf{DIV}} \cdot \mathsf{H}_\rho^{\mathcal{E}\widetilde{\mathcal{F}}}, && \mathsf{B}^{\mathrm{T}} := \mathsf{H}_\rho^{\mathcal{E}\widetilde{\mathcal{F}}} \cdot \mathsf{GRAD}. \end{aligned} \tag{29}$$

The operators B and B^{T} are indeed adjoint and A^{vb} is selfadjoint, owing to the selfadjointness of $\mathsf{H}_\rho^{\mathcal{E}\widetilde{\mathcal{F}}}$ and $\mathsf{H}_\mu^{\mathcal{F}\widetilde{\mathcal{E}}}$ and the discrete adjunctions of GRAD and $\widetilde{\mathsf{DIV}}$ and of CURL and $\widetilde{\mathsf{CURL}}$.

The vertex-based pressure scheme with homogeneous natural BCs is: Find $(\mathbf{p}^*, \mathbf{u}) \in \mathcal{V}_{\perp\mathbf{1}} \times \mathcal{E}$, with $\mathcal{V}_{\perp\mathbf{1}} := \{\boldsymbol{\theta} \in \mathcal{V};\ \left[\!\left[\boldsymbol{\theta}, \mathsf{H}_1^{\mathcal{V}\widetilde{\mathcal{C}}}(\mathbf{1})\right]\!\right]_{\mathcal{V}\widetilde{\mathcal{C}}} = 0\}$, such that

$$\begin{pmatrix} \mathsf{A}^{\mathsf{vb}} & \mathsf{B}^{\mathrm{T}} \\ \mathsf{B} & 0 \end{pmatrix} \begin{pmatrix} \mathbf{u} \\ \mathbf{p}^* \end{pmatrix} = \begin{pmatrix} \mathsf{S}^{\mathsf{vb}}(\rho, \underline{f}^*) \\ 0_{\widetilde{\mathcal{C}}} \end{pmatrix}. \tag{30}$$

The right-hand side $\mathsf{S}^{\mathsf{vb}}(\rho, \underline{f}^*) \in \widetilde{\mathcal{F}}$ discretizes the external load $\rho\underline{f}^*$. Two expressions are considered in the analysis, respectively termed discrete primal and dual load and defined as follows:

$$\mathsf{S}_{\mathsf{p}}^{\mathsf{vb}}(\rho, \underline{f}^*)|_{\tilde{\mathrm{f}}(\mathrm{e})} := (\mathsf{H}_\rho^{\mathcal{E}\widetilde{\mathcal{F}}} \cdot \mathsf{R}_{\mathcal{E}}(\underline{f}^*))|_{\tilde{\mathrm{f}}(\mathrm{e})}, \qquad \mathsf{S}_{\mathsf{d}}^{\mathsf{vb}}(\rho, \underline{f}^*)|_{\tilde{\mathrm{f}}(\mathrm{e})} := \mathsf{R}_{\widetilde{\mathcal{F}}}(\rho\underline{f}^*)|_{\tilde{\mathrm{f}}(\mathrm{e})}, \qquad \forall \mathrm{e} \in \mathrm{E}. \tag{31}$$

A sufficient condition for the discrete primal and dual load to be well-defined is to fix a real number $p \in [1, \infty]$ and to require that $\underline{f}^*$ is in the Sobolev space $W^{s,p}(\Omega)^3$ with $s > \frac{2}{p}$ and $s > \frac{1}{p}$, respectively. For simplicity, we consider the Hilbertian setting and require that $\underline{f}^* \in H^s(\Omega)^3$ with $s > 1$ and $s > \frac{1}{2}$, respectively. Furthermore, non-homogeneous natural BCs can be easily incorporated by modifying the right-hand side of (30) accordingly. We observe that in (30), mass balance holds in each dual cell and momentum balance at each dual face. Specifically,

$$\boldsymbol{\tau}_{\tilde{\mathrm{f}}(\mathrm{e})} + \mathbf{g}_{\tilde{\mathrm{f}}(\mathrm{e})} = \mathsf{S}^{\mathsf{vb}}(\rho, \underline{f}^*)|_{\tilde{\mathrm{f}}(\mathrm{e})}, \qquad \forall \mathrm{e} \in \mathrm{E}, \tag{32a}$$

$$\sum_{\tilde{\mathrm{f}} \in \widetilde{\mathrm{F}}_{\tilde{\mathrm{c}}(\mathrm{v})}} \iota_{\tilde{\mathrm{f}}, \tilde{\mathrm{c}}(\mathrm{v})} \boldsymbol{\phi}_{\tilde{\mathrm{f}}} = 0, \qquad \forall \mathrm{v} \in \mathrm{V}, \tag{32b}$$

with the discrete shear stress $\boldsymbol{\tau} := \widetilde{\mathsf{CURL}}(\boldsymbol{\omega}^*) \in \widetilde{\mathcal{F}}$, the discrete pressure gradient $\mathbf{g} := \mathsf{H}_\rho^{\mathcal{E}\widetilde{\mathcal{F}}} \cdot \mathsf{GRAD}(\mathbf{p}) \in \widetilde{\mathcal{F}}$, and recalling the discrete mass flux $\boldsymbol{\phi} = \mathsf{H}_\rho^{\mathcal{E}\widetilde{\mathcal{F}}}(\mathbf{u}) \in \widetilde{\mathcal{F}}$. All the relations involved in (30) are summarized in Figure 3.

Remark 3.1 (Essential BCs). Essential BCs for (24) are $\underline{u} \times \underline{\nu}_{\partial\Omega} = \underline{u}_\tau^{\mathrm{bc}}$ and $p^* = p^{\mathrm{bc}}$ on $\partial\Omega$. Such BCs can be enforced strongly by removing the corresponding DoFs from the discrete spaces or weakly by a (consistent) penalty method using the full spaces of DoFs. The analysis of vertex-based pressure schemes with essential BCs is left for future work; the main point consists of either deriving suitable discrete Poincaré inequalities on smaller spaces of DoFs if strong enforcement is considered or analyzing the consistency and penalty terms if weak enforcement is considered.

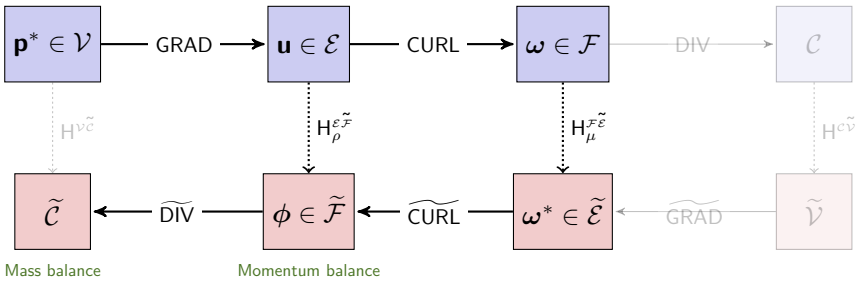

Figure 3: Tonti diagram of the vertex-based pressure scheme for the Stokes equations.

3.2 Stability and well-posedness

Owing to (**A**1) and recalling (19), the norms $\|\cdot\|_{2,\mathcal{E}}$ and $\|\cdot\|_\rho$ are uniformly equivalent on $\mathcal{E}$ (with respect to the mesh size); the same holds for the norms $\|\cdot\|_{2,\mathcal{F}}$ and $\|\cdot\|_\mu$ on $\mathcal{F}$. We equip the space $\mathcal{V}$ with the norm $\|\cdot\|_{2,\mathcal{V}}$ from Lemma 2.1 (obtained by summing cellwise the local norms (17) for vertices).

Lemma 3.1 (Coercivity)**.** *Assume (*$\mathbf{H}_{\mathrm{M}}$*) and (*$\mathbf{H}_{\boldsymbol{\Omega}}$*). Then, there exists* $\eta_{\mathsf{A}} > 0$ *(independent of the mesh size) such that, for all* $\mathbf{u} \in \operatorname{Ker}\mathsf{B}$*, the following inequality holds:*

$$\left[\!\left[\mathbf{u}, \mathsf{A}^{\mathsf{vb}}(\mathbf{u})\right]\!\right]_{\mathcal{E}\widetilde{\mathcal{F}}} \geq \eta_{\mathsf{A}} \|\mathbf{u}\|_\rho^2. \tag{33}$$

Proof. Let us verify that $\mathbf{u} \in \operatorname{Ker}\mathsf{B}$ implies that $\left[\mathbf{u}, \mathsf{H}_\rho^{\mathcal{E}\widetilde{\mathcal{F}}}(\mathbf{v})\right]_{\mathcal{E}\widetilde{\mathcal{F}}} = 0$ for all $\mathbf{v} \in \operatorname{Ker}\mathsf{CURL}$. Owing to ($\mathbf{H}_{\boldsymbol{\Omega}}$) and (7), there is $\boldsymbol{\theta} \in \mathcal{V}$ such that $\mathbf{v} = \mathsf{GRAD}(\boldsymbol{\theta})$. As a result,

$$\left[\!\left[\mathbf{u}, \mathsf{H}_\rho^{\mathcal{E}\widetilde{\mathcal{F}}}(\mathbf{v})\right]\!\right]_{\mathcal{E}\widetilde{\mathcal{F}}} = \left[\!\left[\mathbf{u}, \mathsf{B}^{\mathrm{T}}(\boldsymbol{\theta})\right]\!\right]_{\mathcal{E}\widetilde{\mathcal{F}}} = \left[\!\left[\boldsymbol{\theta}, \mathsf{B}(\mathbf{u})\right]\!\right]_{\mathcal{V}\widetilde{\mathcal{C}}} = 0.$$

Applying Lemma 2.2 and the stability property (19), we infer that

$$\eta_\rho \|\mathbf{u}\|_\rho^2 \leq \|\mathbf{u}\|_{2,\mathcal{E}}^2 \leq (C_{\mathrm{P}}^{(1)})^2 \|\mathsf{CURL}(\mathbf{u})\|_{2,\mathcal{F}}^2 \leq (C_{\mathrm{P}}^{(1)})^2 \eta_\mu^{-1} \|\mathsf{CURL}(\mathbf{u})\|_\mu^2,$$

whence we infer (33) with $\eta_{\mathsf{A}} = \eta_\rho \eta_\mu (C_{\mathrm{P}}^{(1)})^{-2}$ since $\|\mathsf{CURL}(\mathbf{u})\|_\mu^2 = \left[\!\left[\mathbf{u}, \mathsf{A}^{\mathsf{vb}}(\mathbf{u})\right]\!\right]_{\mathcal{E}\widetilde{\mathcal{F}}}$. □

Lemma 3.2 (Discrete inf-sup condition)**.** *Assume (*$\mathbf{H}_{\mathrm{M}}$*). Then, there exists* $\beta_{\mathsf{B}} > 0$ *(independent of the mesh size) such that*

$$\inf_{\boldsymbol{\theta} \in \mathcal{V}_{\perp \mathbf{1}}} \sup_{\mathbf{u} \in \mathcal{E}} \frac{\left[\!\left[\boldsymbol{\theta}, \mathsf{B}(\mathbf{u})\right]\!\right]_{\mathcal{V}\widetilde{\mathcal{C}}}}{\|\boldsymbol{\theta}\|_{2,\mathcal{V}} \|\mathbf{u}\|_\rho} \geq \beta_{\mathsf{B}}. \tag{34}$$

Proof. For all $\boldsymbol{\theta} \in \mathcal{V}_{\perp \mathbf{1}}$, set $\mathbf{u} := \mathsf{GRAD}(\boldsymbol{\theta})$. Then, $\left[\!\left[\boldsymbol{\theta}, \mathsf{B}(\mathbf{u})\right]\!\right]_{\mathcal{V}\widetilde{\mathcal{C}}} = \left[\!\left[\mathbf{u}, \mathsf{B}^{\mathrm{T}}(\boldsymbol{\theta})\right]\!\right]_{\mathcal{E}\widetilde{\mathcal{F}}} = \|\mathbf{u}\|_\rho^2$ and owing to Lemma 2.1 and (**A**1), we infer that $\|\boldsymbol{\theta}\|_{2,\mathcal{V}} \leq C_{\mathrm{P}}^{(0)} \eta_\rho^{-1/2} \|\mathbf{u}\|_\rho$. This yields the inf-sup condition with $\beta_{\mathsf{B}} = \eta_\rho^{1/2} (C_{\mathrm{P}}^{(0)})^{-1}$. □

A classical consequence of Lemmata 3.1 and 3.2 is the following [15]:

Corollary 3.3 (Well-posedness)**.** *Assume (*$\mathbf{H}_{\mathrm{M}}$*) and (*$\mathbf{H}_{\boldsymbol{\Omega}}$*). Then, the discrete system* (30) *is well-posed.*

3.3 Error analysis for discrete dual load

Let $\underline{u}$, p^* solve the 2-field curl formulation (24) and recall that $\underline{\omega} = \underline{\mathrm{curl}}(\underline{u})$. Let $\mathbf{u}$, $\mathbf{p}^*$ solve the discrete system (30) and recall that $\boldsymbol{\omega} = \mathsf{CURL}(\mathbf{u})$. We define the following discrete errors:

$$\boldsymbol{\delta}\mathbf{p}^* := \mathsf{R}_{\mathcal{V}}(p^*) - \mathbf{p}^*, \quad \boldsymbol{\delta}\mathbf{u} := \mathsf{R}_{\mathcal{E}}(\underline{u}) - \mathbf{u}, \quad \boldsymbol{\delta}\boldsymbol{\omega} := \mathsf{R}_{\mathcal{F}}(\underline{\omega}) - \boldsymbol{\omega}. \tag{35}$$

Recall the global commuting operators $\lfloor \rho, {}_{\mathcal{E}}\widetilde{\mathcal{F}} \rceil(\bullet) := \mathsf{H}_\rho^{\mathcal{E}\widetilde{\mathcal{F}}} \cdot \mathsf{R}_{\mathcal{E}}(\bullet) - \mathsf{R}_{\widetilde{\mathcal{F}}}(\rho\bullet)$ and $\lfloor \mu, {}_{\mathcal{F}}\widetilde{\mathcal{E}} \rceil(\bullet) := \mathsf{H}_\mu^{\mathcal{F}\widetilde{\mathcal{E}}} \cdot \mathsf{R}_{\mathcal{F}}(\bullet) - \mathsf{R}_{\widetilde{\mathcal{E}}}(\mu\bullet)$. For simplicity, we assume that there are no quadrature errors when evaluating the external load.

Theorem 3.4 (Error bounds with discrete dual load)**.** *Let $\underline{u}$, p^* solve of the 2-field curl formulation* (24) *with homogeneous natural BCs. Let* $\mathbf{u}$, $\mathbf{p}^*$ *solve the discrete system* (30) *with the discrete dual load* $\mathsf{S}_{\mathsf{d}}^{\mathsf{vb}}(\rho, \underline{f}^*)$ *with* $\underline{f}^* \in H^s(\Omega)^3$, $s > \frac{1}{2}$. *Assume* ($\mathbf{H}_{\mathrm{M}}$) *and* ($\mathbf{H}_{\mathbf{\Omega}}$). *Then, the following error bounds hold:*

$$\|\mathsf{GRAD}(\boldsymbol{\delta}\mathbf{p}^*)\|_\rho \le \|\lfloor \rho,\, \varepsilon^{\tilde{\mathcal{F}}}\rceil(\underline{\mathrm{grad}}(p^*))\|_{\rho^{-1}}, \tag{36a}$$

$$\|\boldsymbol{\delta\omega}\|_\mu \lesssim \|\lfloor \rho,\, \varepsilon^{\tilde{\mathcal{F}}}\rceil(\underline{\mathrm{grad}}(p^*))\|_{\rho^{-1}} + \|\lfloor \mu,\, {}^{\mathcal{F}}\tilde{\varepsilon}\rceil(\underline{\omega})\|_{\mu^{-1}}, \tag{36b}$$

$$\|\boldsymbol{\delta}\mathbf{u}\|_\rho \lesssim \|\lfloor \rho,\, \varepsilon^{\tilde{\mathcal{F}}}\rceil(\underline{\mathrm{grad}}(p^*))\|_{\rho^{-1}} + \|\lfloor \mu,\, {}^{\mathcal{F}}\tilde{\varepsilon}\rceil(\underline{\omega})\|_{\mu^{-1}} + \|\lfloor \rho,\, \varepsilon^{\tilde{\mathcal{F}}}\rceil(\underline{u})\|_{\rho^{-1}}. \tag{36c}$$

Moreover, if $\underline{u}, \underline{\omega}, \underline{\mathrm{grad}}(p^*) \in [H^1(\mathrm{C})]^3$ *and* $\underline{f}^* \in [L^4(\Omega)]^3$, *the following error bounds hold:*

$$\|\mathsf{GRAD}(\boldsymbol{\delta}\mathbf{p}^*)\|_\rho \lesssim h_{\mathrm{M}}\, \|\underline{\mathrm{grad}}(p^*)\|_{[H^1(\mathrm{C})]^3}, \tag{37a}$$

$$\|\boldsymbol{\delta\omega}\|_\mu \lesssim h_{\mathrm{M}} \left(\|\underline{\mathrm{grad}}(p^*)\|_{[H^1(\mathrm{C})]^3} + \|\underline{\omega}\|_{[H^1(\mathrm{C})]^3} + \|\underline{f}^*\|_{[L^4(\Omega)]^3}\right), \tag{37b}$$

$$\|\boldsymbol{\delta}\mathbf{u}\|_\rho \lesssim h_{\mathrm{M}} \left(\|\underline{\mathrm{grad}}(p^*)\|_{[H^1(\mathrm{C})]^3} + \|\underline{\omega}\|_{[H^1(\mathrm{C})]^3} + \|\underline{f}^*\|_{[L^4(\Omega)]^3} + \|\underline{u}\|_{[H^1(\mathrm{C})]^3}\right). \tag{37c}$$

Proof. (1) We first derive the error equations. Applying $\mathsf{R}_{\widetilde{\mathcal{F}}}$ to the momentum and $\mathsf{R}_{\widetilde{\mathcal{C}}}$ to the mass balance equation in (24) yields

$$\widetilde{\mathsf{CURL}}(\mathsf{R}_{\widetilde{\mathcal{E}}}(\mu\underline{\omega})) + \mathsf{R}_{\widetilde{\mathcal{F}}}(\rho\,\underline{\mathrm{grad}}(p^*)) = \mathsf{S}_{\mathsf{d}}^{\mathsf{vb}}(\rho, \underline{f}^*),$$
$$\widetilde{\mathsf{DIV}}(\mathsf{R}_{\widetilde{\mathcal{F}}}(\rho\underline{u})) = 0_{\widetilde{\mathcal{C}}},$$

owing to the commuting property (9) on the interior dual mesh entities and the homogeneous BCs (25) on the dual mesh entities touching the boundary $\partial\Omega$. Subtracting from the corresponding equation in (30) and introducing the global commuting operators leads to

$$\widetilde{\mathsf{CURL}} \cdot \mathsf{H}_\mu^{{}^{\mathcal{F}}\tilde{\varepsilon}}(\boldsymbol{\delta\omega}) + \mathsf{H}_\rho^{\varepsilon^{\tilde{\mathcal{F}}}} \cdot \mathsf{GRAD}(\boldsymbol{\delta}\mathbf{p}^*) = \widetilde{\mathsf{CURL}}(\lfloor \mu,\, {}^{\mathcal{F}}\tilde{\varepsilon}\rceil(\underline{\omega})) + \lfloor \rho,\, \varepsilon^{\tilde{\mathcal{F}}}\rceil(\underline{\mathrm{grad}}(p^*)), \tag{38a}$$

$$\widetilde{\mathsf{DIV}} \cdot \mathsf{H}_\rho^{\varepsilon^{\tilde{\mathcal{F}}}}(\boldsymbol{\delta}\mathbf{u}) = \widetilde{\mathsf{DIV}}(\lfloor \rho,\, \varepsilon^{\tilde{\mathcal{F}}}\rceil(\underline{u})), \tag{38b}$$

since $\mathsf{R}_{\mathcal{E}}(\underline{\mathrm{grad}}(p^*)) = \mathsf{GRAD}(\mathsf{R}_{\mathcal{V}}(p^*))$.
(2) Bound on the pressure gradient. We take the duality product of (38a) with $\mathsf{GRAD}(\boldsymbol{\delta}\mathbf{p}^*)$. Since $\big[\!\big[\mathsf{GRAD}(\boldsymbol{\delta}\mathbf{p}^*), \widetilde{\mathsf{CURL}}(\mathbf{x})\big]\!\big]_{\varepsilon^{\tilde{\mathcal{F}}}} = \big[\!\big[\mathsf{CURL}(\mathsf{GRAD}(\boldsymbol{\delta}\mathbf{p}^*)), \mathbf{x}\big]\!\big]_{{}^{\mathcal{F}}\tilde{\mathcal{E}}} = 0$ for all $\mathbf{x} \in \widetilde{\mathcal{E}}$, we infer that $\|\mathsf{GRAD}(\boldsymbol{\delta}\mathbf{p}^*)\|_\rho^2 = \big[\!\big[\mathsf{GRAD}(\boldsymbol{\delta}\mathbf{p}^*), \lfloor \rho,\, \varepsilon^{\tilde{\mathcal{F}}}\rceil(\underline{\mathrm{grad}}(p^*))\big]\!\big]_{\varepsilon^{\tilde{\mathcal{F}}}}$, whence (36a) follows from the Cauchy–Schwarz inequality (28).
(3) Bound on the vorticity. We use the discrete Hodge decomposition

$$\mathcal{E} = \mathrm{Im}\,\mathsf{GRAD} \overset{\perp\mathsf{H}}{\oplus} (\mathrm{Ker}\,\mathsf{CURL})^{\perp\mathsf{H}}, \tag{39}$$

where $(\mathrm{Ker}\,\mathsf{CURL})^{\perp\mathsf{H}} := \{\mathbf{u} \in \mathcal{E};\ \big[\mathbf{u}, \mathsf{H}_\rho^{\varepsilon^{\tilde{\mathcal{F}}}}(\mathbf{v})\big]_{\varepsilon^{\tilde{\mathcal{F}}}} = 0, \forall \mathbf{v} \in \mathrm{Ker}\,\mathsf{CURL}\}$, which results from the decomposition $\mathcal{E} = \mathrm{Im}\,\mathsf{GRAD} \overset{\perp\mathsf{H}}{\oplus} (\mathrm{Im}\,\mathsf{GRAD})^{\perp\mathsf{H}}$ and $\mathrm{Im}\,\mathsf{GRAD} = \mathrm{Ker}\,\mathsf{CURL}$ owing to ($\mathbf{H}_{\mathbf{\Omega}}$) and (7). Using (39), we set $\boldsymbol{\delta}\mathbf{u} = \mathsf{GRAD}(\boldsymbol{\delta\theta}) + \boldsymbol{\delta}\mathbf{u}_\perp$ with $\boldsymbol{\delta\theta} \in \mathcal{V}$ and $\boldsymbol{\delta}\mathbf{u}_\perp \in (\mathrm{Ker}\,\mathsf{CURL})^{\perp\mathsf{H}}$. Observe that $\mathsf{CURL}(\boldsymbol{\delta}\mathbf{u}_\perp) = \mathsf{CURL}(\boldsymbol{\delta}\mathbf{u}) = \boldsymbol{\delta\omega}$ and that $\|\boldsymbol{\delta}\mathbf{u}_\perp\|_\rho \lesssim \|\boldsymbol{\delta\omega}\|_\mu$ owing to Lemma 2.2 and the stability of $\mathsf{H}_\rho^{\varepsilon^{\tilde{\mathcal{F}}}}$ and $\mathsf{H}_\mu^{{}^{\mathcal{F}}\tilde{\varepsilon}}$. We take the duality product of (38a) with $\boldsymbol{\delta}\mathbf{u}_\perp$. Since $\big[\!\big[\boldsymbol{\delta}\mathbf{u}_\perp, \mathsf{H}_\rho^{\varepsilon^{\tilde{\mathcal{F}}}} \cdot \mathsf{GRAD}(\boldsymbol{\delta}\mathbf{p}^*)\big]\!\big]_{\varepsilon^{\tilde{\mathcal{F}}}} = 0$, we infer that

$$\|\boldsymbol{\delta\omega}\|_\mu^2 = \big[\!\big[\boldsymbol{\delta\omega}, \lfloor \mu,\, {}^{\mathcal{F}}\tilde{\varepsilon}\rceil(\underline{\omega})\big]\!\big]_{{}^{\mathcal{F}}\tilde{\mathcal{E}}} + \big[\!\big[\boldsymbol{\delta}\mathbf{u}_\perp, \lfloor \rho,\, \varepsilon^{\tilde{\mathcal{F}}}\rceil(\underline{\mathrm{grad}}(p^*))\big]\!\big]_{\varepsilon^{\tilde{\mathcal{F}}}}. \tag{40}$$

The estimate (36b) results from Cauchy–Schwarz inequalities and $\|\boldsymbol{\delta}\mathbf{u}_\perp\|_\rho \lesssim \|\boldsymbol{\delta\omega}\|_\mu$.
(4) Bound on the velocity. Since $\|\boldsymbol{\delta}\mathbf{u}\|_\rho^2 = \|\boldsymbol{\delta}\mathbf{u}_\perp\|_\rho^2 + \|\mathsf{GRAD}(\boldsymbol{\delta\theta})\|_\rho^2$ and $\|\boldsymbol{\delta}\mathbf{u}_\perp\|_\rho \lesssim \|\boldsymbol{\delta\omega}\|_\mu$, it remains to estimate $\|\mathsf{GRAD}(\boldsymbol{\delta\theta})\|_\rho$. We take the duality product of (38b) with $\boldsymbol{\delta\theta}$. Since $\big[\boldsymbol{\delta}\mathbf{u}_\perp, \mathsf{H}_\rho^{\varepsilon^{\tilde{\mathcal{F}}}} \cdot \mathsf{GRAD}(\boldsymbol{\delta\theta})\big]\!\big]_{\varepsilon^{\tilde{\mathcal{F}}}} = 0$, we infer that

$$\|\mathsf{GRAD}(\boldsymbol{\delta\theta})\|_\rho^2 = \big[\!\big[\mathsf{GRAD}(\boldsymbol{\delta\theta}), \mathsf{H}_\rho^{\varepsilon^{\tilde{\mathcal{F}}}}(\boldsymbol{\delta}\mathbf{u})\big]\!\big]_{\varepsilon^{\tilde{\mathcal{F}}}} = \big[\!\big[\mathsf{GRAD}(\boldsymbol{\delta\theta}), \lfloor \rho,\, \varepsilon^{\tilde{\mathcal{F}}}\rceil(\underline{u})\big]\!\big]_{\varepsilon^{\tilde{\mathcal{F}}}},$$

and the Cauchy–Schwarz inequality (28) yields $\|\mathsf{GRAD}(\boldsymbol{\delta\theta})\|_\rho \le \|\lfloor \rho,\, \varepsilon^{\tilde{\mathcal{F}}}\rceil(\underline{u})\|_{\rho^{-1}}$.
(5) Finally, the error bounds for smooth solutions result from Lemma 2.3, observing in particular that $\underline{\mathrm{curl}}(\underline{\omega}) \in [L^4(\Omega)]^3$ since $\underline{\mathrm{curl}}(\underline{\omega}) = \underline{f}^* - \underline{\mathrm{grad}}(p^*)$, $\underline{f}^* \in [L^4(\Omega)]^3$, and $\underline{\mathrm{grad}}(p^*) \in [H^1(\mathrm{C})]^3$, and that $\underline{\mathrm{curl}}(\underline{u}) \in [L^4(\Omega)]^3$ since $\underline{\omega} = \underline{\mathrm{curl}}(\underline{u}) \in [H^1(\mathrm{C})]^3$. □

3.4 Error analysis for discrete primal load

Theorem 3.5 (Error bounds with discrete primal load)**.** *Let $\underline{u}$, p^* solve of the 2-field curl formulation* (24) *with homogeneous natural BCs. Let* $\mathbf{u}$, $\mathbf{p}^*$ *solve the discrete system* (30) *with the discrete primal load $\mathsf{S}_{\mathsf{p}}^{\mathsf{vb}}(\rho, \underline{f}^*)$ with $\underline{f}^* \in H^s(\Omega)^3$, $s > 1$. Assume (*$\mathbf{H}_{\mathrm{M}}$*) and (*$\mathbf{H}_{\mathbf{\Omega}}$*). Then, the following error bounds hold:*

$$\|\mathsf{GRAD}(\boldsymbol{\delta}\mathbf{p}^*)\|_\rho \le \|\lfloor \rho,\, \varepsilon\tilde{\mathcal{F}}\rceil(\underline{\mathrm{curl}}(\underline{\omega}^*))\|_{\rho^{-1}}, \tag{41a}$$

$$\|\boldsymbol{\delta}\boldsymbol{\omega}\|_\mu \lesssim \|\lfloor \rho,\, \varepsilon\tilde{\mathcal{F}}\rceil(\underline{\mathrm{curl}}(\underline{\omega}^*))\|_{\rho^{-1}} + \|\lfloor \mu,\, \mathcal{F}\tilde{\varepsilon}\rceil(\underline{\omega})\|_{\mu^{-1}}, \tag{41b}$$

$$\|\boldsymbol{\delta}\mathbf{u}\|_\rho \lesssim \|\lfloor \rho,\, \varepsilon\tilde{\mathcal{F}}\rceil(\underline{\mathrm{curl}}(\underline{\omega}^*))\|_{\rho^{-1}} + \|\lfloor \mu,\, \mathcal{F}\tilde{\varepsilon}\rceil(\underline{\omega})\|_{\mu^{-1}} + \|\lfloor \rho,\, \varepsilon\tilde{\mathcal{F}}\rceil(\underline{u})\|_{\rho^{-1}}. \tag{41c}$$

Moreover, if $\underline{u}, \underline{\omega}, \underline{\mathrm{curl}}(\underline{\omega}^*) \in [H^1(\mathrm{C})]^3$ and $\underline{\mathrm{curl}}(\underline{f}^*) \in [L^4(\Omega)]^3$, the following error bounds hold:

$$\|\mathsf{GRAD}(\boldsymbol{\delta}\mathbf{p}^*)\|_\rho \lesssim h_{\mathrm{M}} \left(\|\underline{\mathrm{curl}}(\underline{\omega}^*)\|_{[H^1(\mathrm{C})]^3} + \|\underline{\mathrm{curl}}\, \underline{f}^*\|_{[L^4(\Omega)]^3}\right), \tag{42a}$$

$$\|\boldsymbol{\delta}\boldsymbol{\omega}\|_\mu \lesssim h_{\mathrm{M}} \left(\|\underline{\mathrm{curl}}(\underline{\omega}^*)\|_{[H^1(\mathrm{C})]^3} + \|\underline{\mathrm{curl}}\, \underline{f}^*\|_{[L^4(\Omega)]^3} + \|\underline{\omega}\|_{[H^1(\mathrm{C})]^3}\right), \tag{42b}$$

$$\|\boldsymbol{\delta}\mathbf{u}\|_\rho \lesssim h_{\mathrm{M}} \left(\|\underline{\mathrm{curl}}(\underline{\omega}^*)\|_{[H^1(\mathrm{C})]^3} + \|\underline{\mathrm{curl}}\, \underline{f}^*\|_{[L^4(\Omega)]^3} + \|\underline{\omega}\|_{[H^1(\mathrm{C})]^3} + \|\underline{u}\|_{[H^1(\mathrm{C})]^3}\right). \tag{42c}$$

Proof. Since $\mathsf{S}_{\mathsf{p}}^{\mathsf{vb}}(\rho, \underline{f}^*) = \mathsf{S}_{\mathsf{d}}^{\mathsf{vb}}(\rho, \underline{f}^*) + \lfloor \rho,\, \varepsilon\tilde{\mathcal{F}}\rceil(\underline{f}^*)$, the main difference with the proof of Theorem 3.4 is that the error equation (38a) is to be replaced by

$$\widetilde{\mathsf{CURL}} \cdot \mathsf{H}_\mu^{\mathcal{F}\tilde{\varepsilon}} \cdot \mathsf{CURL}(\boldsymbol{\delta}\mathbf{u}) + \mathsf{H}_\rho^{\varepsilon\tilde{\mathcal{F}}} \cdot \mathsf{GRAD}(\boldsymbol{\delta}\mathbf{p}^*) = \widetilde{\mathsf{CURL}}(\lfloor \mu,\, \mathcal{F}\tilde{\varepsilon}\rceil(\underline{\omega})) - \lfloor \rho,\, \varepsilon\tilde{\mathcal{F}}\rceil(\underline{\mathrm{curl}}(\underline{\omega}^*)).$$

The rest of the proof follows along similar lines, and is skipped for brevity. □

Remark 3.2 (Comparison with Theorem 3.4). When the divergence-free part of the external load (i.e., $\underline{\mathrm{curl}}(\underline{\omega}^*)$) is expected to dominate over the curl-free part (i.e., $\underline{\mathrm{grad}}(p^*)$), using a discrete dual load is more appropriate since the error bounds do not depend on $\underline{\mathrm{curl}}(\underline{\omega}^*)$. Alternatively, when the curl-free part is expected to dominate over the divergence-free part, using a discrete primal load is more appropriate since the error bounds do not depend on $\underline{\mathrm{grad}}(p^*)$.

4 Cell-Based Pressure Schemes

4.1 Discrete systems

Cell-based pressure schemes rely on the 3-field curl formulation (2). Introducing the mass density ρ and the viscosity μ leads to

$$\begin{cases} -\mu^{-1}\underline{\omega}^* + \underline{\mathrm{curl}}(\rho^{-1}\underline{\phi}) = \underline{0}, & \text{in } \Omega, \\ \rho^{-1}\,\underline{\mathrm{curl}}(\underline{\omega}^*) + \underline{\mathrm{grad}}(p^*) = \underline{f}^*, & \text{in } \Omega, \\ \mathrm{div}(\underline{\phi}) = 0, & \text{in } \Omega, \end{cases} \tag{43}$$

recalling that $\underline{\phi} = \rho\underline{u}$, $\underline{\omega} = \underline{\mathrm{curl}}(\underline{u})$, $\underline{\omega}^* = \mu\underline{\omega}$, and $p^* = \rho^{-1}p$. We focus on natural BCs for (43), which are given by

$$\underline{u} \times \underline{\nu}_{\partial\Omega} = \underline{u}_\tau^{\mathrm{bc}}, \quad p^* = p^{\mathrm{bc}}, \qquad \text{on } \partial\Omega, \tag{44}$$

with data $\underline{u}_\tau^{\mathrm{bc}}$ and p^{bc}. A discussion similar to that in Remark 3.1 can be made regarding essential BCs.

In cell-based pressure schemes, the DoFs of the pressure potential, denoted $\mathbf{p}^*$, are located at dual mesh vertices (in one-to-one pairing with primal mesh cells). The DoFs of the mass flux, denoted $\boldsymbol{\phi}$, are located at primal faces, while the DoFs of the viscous stress circulation, denoted $\boldsymbol{\omega}^*$, are located at primal edges. There are two discrete Hodge operators, one related to the (reciprocal of) the mass density ρ and the other to the (reciprocal of) the viscosity μ. The discrete Hodge operator $\mathsf{H}_{\rho^{-1}}^{\mathcal{F}\tilde{\varepsilon}}$ links the discrete velocity and mass flux in the form $\mathbf{u} = \mathsf{H}_{\rho^{-1}}^{\mathcal{F}\tilde{\varepsilon}}(\boldsymbol{\phi}) \in \widetilde{\mathcal{E}}$ (compare with $\underline{u} = \rho^{-1}\underline{\phi}$), while the

discrete Hodge operator $\mathsf{H}^{\varepsilon\widetilde{\mathcal{F}}}_{\mu^{-1}}$ links the discrete vorticity to the discrete viscous stress circulation in the form $\boldsymbol{\omega} = \mathsf{H}^{\varepsilon\widetilde{\mathcal{F}}}_{\mu^{-1}}(\boldsymbol{\omega}^*) \in \widetilde{\mathcal{F}}$ (compare with $\underline{\omega} = \mu^{-1}\underline{\omega}^*$). Both discrete Hodge operators are assumed to satisfy the stability and $\mathbb{P}_0$-consistency properties (**A**1) and (**A**2). In what follows, we consider the following discrete norms:

$$\|\boldsymbol{\phi}\|^2_{\rho^{-1}} := \left[\!\left[\boldsymbol{\phi}, \mathsf{H}^{\mathcal{F}\widetilde{\mathcal{E}}}_{\rho^{-1}}(\boldsymbol{\phi})\right]\!\right]_{\mathcal{F}\widetilde{\mathcal{E}}}, \qquad \|\mathbf{u}\|^2_{\rho} := \left[\!\left[(\mathsf{H}^{\mathcal{F}\widetilde{\mathcal{E}}}_{\rho^{-1}})^{-1}(\mathbf{u}), \mathbf{u}\right]\!\right]_{\mathcal{F}\widetilde{\mathcal{E}}}, \tag{45a}$$

$$\|\boldsymbol{\omega}^*\|^2_{\mu^{-1}} := \left[\!\left[\boldsymbol{\omega}^*, \mathsf{H}^{\mathcal{E}\widetilde{\mathcal{F}}}_{\mu^{-1}}(\boldsymbol{\omega}^*)\right]\!\right]_{\mathcal{E}\widetilde{\mathcal{F}}}, \qquad \|\boldsymbol{\omega}\|^2_{\mu} := \left[\!\left[(\mathsf{H}^{\mathcal{E}\widetilde{\mathcal{F}}}_{\mu^{-1}})^{-1}(\boldsymbol{\omega}), \boldsymbol{\omega}\right]\!\right]_{\mathcal{E}\widetilde{\mathcal{F}}}, \tag{45b}$$

for all $\boldsymbol{\phi} \in \mathcal{F}$, $\mathbf{u} \in \widetilde{\mathcal{E}}$, $\boldsymbol{\omega}^* \in \mathcal{E}$, and $\boldsymbol{\omega} \in \widetilde{\mathcal{F}}$. Note that these norms differ from those defined in (27) for vertex-based pressure schemes. Owing to the Cauchy–Schwarz inequality, we infer that

$$\left[\!\left[\boldsymbol{\phi}, \mathbf{u}\right]\!\right]_{\mathcal{F}\widetilde{\mathcal{E}}} \le \|\boldsymbol{\phi}\|_{\rho^{-1}} \|\mathbf{u}\|_{\rho}, \qquad \left[\!\left[\boldsymbol{\omega}^*, \boldsymbol{\omega}\right]\!\right]_{\mathcal{E}\widetilde{\mathcal{F}}} \le \|\boldsymbol{\omega}^*\|_{\mu^{-1}} \|\boldsymbol{\omega}\|_{\mu}. \tag{46}$$

We introduce the following operators:

$$\begin{aligned} &\mathsf{A}^{\mathsf{cb}} : \mathcal{E} \to \widetilde{\mathcal{F}}, \quad &&\mathsf{C} : \mathcal{E} \to \widetilde{\mathcal{E}}, \quad &&\mathsf{C}^{\mathrm{T}} : \mathcal{F} \to \widetilde{\mathcal{F}}, \quad &&\mathsf{D} : \mathcal{F} \to \mathcal{C}, \quad &&\mathsf{D}^{\mathrm{T}} : \widetilde{\mathcal{V}} \to \widetilde{\mathcal{E}}, \\ &\mathsf{A}^{\mathsf{cb}} := -\mathsf{H}^{\mathcal{E}\widetilde{\mathcal{F}}}_{\mu^{-1}}, \quad &&\mathsf{C} := \mathsf{H}^{\mathcal{F}\widetilde{\mathcal{E}}}_{\rho^{-1}} \cdot \mathsf{CURL}, \quad &&\mathsf{C}^{\mathrm{T}} := \widetilde{\mathsf{CURL}} \cdot \mathsf{H}^{\mathcal{F}\widetilde{\mathcal{E}}}_{\rho^{-1}}, \quad &&\mathsf{D} := -\mathsf{DIV}, \quad &&\mathsf{D}^{\mathrm{T}} := \widetilde{\mathsf{GRAD}}. \end{aligned} \tag{47}$$

The operators C (resp. D) and C^{T} (resp. D^{T}) are adjoint owing to the adjunction property (13) and the selfadjointness of $\mathsf{H}^{\mathcal{F}\widetilde{\mathcal{E}}}_{\rho^{-1}}$; moreover, A^{cb} is selfadjoint and negative definite.

The cell-based pressure scheme with homogeneous natural BCs is: Find $(\mathbf{p}^*, \boldsymbol{\phi}, \boldsymbol{\omega}^*) \in \widetilde{\mathcal{V}} \times \mathcal{F} \times \mathcal{E}$ such that

$$\begin{pmatrix} \mathsf{A}^{\mathsf{cb}} & \mathsf{C}^{\mathrm{T}} & 0 \\ \mathsf{C} & 0 & \mathsf{D}^{\mathrm{T}} \\ 0 & \mathsf{D} & 0 \end{pmatrix} \begin{pmatrix} \boldsymbol{\omega}^* \\ \boldsymbol{\phi} \\ \mathbf{p}^* \end{pmatrix} = \begin{pmatrix} 0_{\widetilde{\mathcal{F}}} \\ \mathsf{S}^{\mathsf{cb}}(\rho, \underline{f}^*) \\ 0_{\mathcal{C}} \end{pmatrix}. \tag{48}$$

The right-hand side $\mathsf{S}^{\mathsf{cb}}(\rho, \underline{f}^*) \in \widetilde{\mathcal{E}}$ discretizes the external load $\underline{f}^*$. Two expressions are considered in the analysis, respectively termed discrete primal and dual load and defined as follows:

$$\mathsf{S}^{\mathsf{cb}}_{\mathsf{p}}(\rho, \underline{f}^*)|_{\tilde{\mathrm{e}}(\mathrm{f})} := \left(\mathsf{H}^{\mathcal{F}\widetilde{\mathcal{E}}}_{\rho^{-1}} \cdot \mathsf{R}_{\mathcal{F}}(\rho \underline{f}^*)\right)|_{\tilde{\mathrm{e}}(\mathrm{f})}, \qquad \mathsf{S}^{\mathsf{cb}}_{\mathsf{d}}(\rho, \underline{f}^*)|_{\tilde{\mathrm{e}}(\mathrm{f})} := \mathsf{R}_{\widetilde{\mathcal{E}}}(\underline{f}^*)|_{\tilde{\mathrm{e}}(\mathrm{f})}, \qquad \forall \mathrm{f} \in \mathrm{F}. \tag{49}$$

A sufficient condition for the discrete primal and dual load to be well-defined is to require that $\underline{f}^* \in H^s(\Omega)^3$ with $s > \frac{1}{2}$ and $s > 1$, respectively. Furthermore, non-homogeneous natural BCs can be easily incorporated by modifying the right-hand side of (48) accordingly. We observe that in (48), mass balance holds in each primal cell and momentum balance at each dual edge; moreover, $\boldsymbol{\omega} = \widetilde{\mathsf{CURL}}(\mathbf{u})$ holds. Specifically,

$$\boldsymbol{\tau}_{\tilde{\mathrm{e}}(\mathrm{f})} + \mathbf{g}_{\tilde{\mathrm{e}}(\mathrm{f})} = \mathsf{S}^{\mathsf{cb}}(\rho, \underline{f}^*)|_{\tilde{\mathrm{e}}(\mathrm{f})}, \qquad \forall \mathrm{f} \in \mathrm{F}, \tag{50a}$$

$$\sum_{\mathrm{f} \in \mathrm{F}_{\mathrm{c}}} \iota_{\mathrm{f},\mathrm{c}} \boldsymbol{\phi}_{\mathrm{f}} = 0, \qquad \forall \mathrm{c} \in \mathrm{C}, \tag{50b}$$

with the discrete shear stress $\boldsymbol{\tau} := \mathsf{H}^{\mathcal{F}\widetilde{\mathcal{E}}}_{\rho^{-1}} \cdot \mathsf{CURL}(\boldsymbol{\omega}^*) \in \widetilde{\mathcal{E}}$ and the discrete pressure gradient $\mathbf{g} := \widetilde{\mathsf{GRAD}}(\mathbf{p}) \in \widetilde{\mathcal{E}}$. All the relations involved in (48) are summarized in Figure 4.

4.2 Stability and well-posedness

Owing to (**A**1) and recalling (19), the norms $\|\cdot\|_{2,\mathcal{E}}$ and $\|\cdot\|_{\mu^{-1}}$ are uniformly equivalent on $\mathcal{E}$ (with respect to the mesh size); the same holds for the norms $\|\cdot\|_{2,\mathcal{F}}$ and $\|\cdot\|_{\rho^{-1}}$ on $\mathcal{F}$. We equip $\widetilde{\mathcal{V}}$ with the norm $\|\mathbf{p}\|^2_{2,\widetilde{\mathcal{V}}} := \sum_{\mathrm{c} \in \mathrm{C}} |\mathrm{c}| (\mathbf{p}_{\tilde{\mathrm{v}}(\mathrm{c})})^2$ and $\widetilde{\mathcal{E}}$ with the norm $\|\mathbf{g}\|^2_{2,\widetilde{\mathcal{E}}} := \sum_{\mathrm{c} \in \mathrm{C}} \sum_{\mathrm{f} \in \mathrm{F}_{\mathrm{c}}} |\mathfrak{p}_{\mathrm{f},\mathrm{c}}| (\frac{\mathbf{g}_{\tilde{\mathrm{e}}(\mathrm{f})}}{|\tilde{\mathrm{e}}(\mathrm{f})|})^2$ where $\mathfrak{p}_{\mathrm{f},\mathrm{c}}$ is

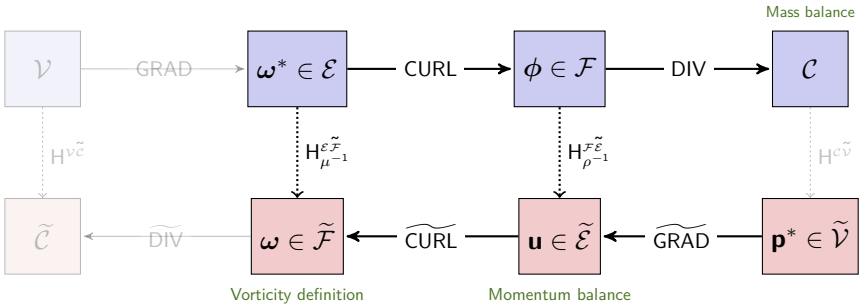

Figure 4: Tonti diagram of the cell-based pressure scheme for the Stokes equations.

illustrated in Figure 2. Under assumption ($\mathbf{H}_{\mathrm{M}}$), the following discrete Poincaré inequality is proved in [11]: There exists $C_{\mathrm{P}}^{(\tilde{0})}$ such that, for all $\mathbf{p} \in \widetilde{\mathcal{V}}$,

$$\|\mathbf{p}\|_{2,\widetilde{\mathcal{V}}} \le C_{\mathrm{P}}^{(\tilde{0})} \|\widetilde{\mathsf{GRAD}}(\mathbf{p})\|_{2,\widetilde{\mathcal{E}}}. \tag{51}$$

Lemma 4.1 (Discrete inf-sup conditions)**.** *Assume ($\mathbf{H}_{\mathrm{M}}$) and ($\mathbf{H}_{\boldsymbol{\Omega}}$). Then, there exist $\beta_{\mathsf{C}} > 0$ and $\beta_{\mathsf{D}} > 0$ (independent of the mesh size) such that*

$$\inf_{\mathbf{p}\in\widetilde{\mathcal{V}}} \sup_{\mathbf{v}\in\mathcal{F}} \frac{[\![\mathsf{D}(\mathbf{v}),\mathbf{p}]\!]_{c\tilde{\nu}}}{\|\mathbf{p}\|_{2,\widetilde{\mathcal{V}}}\|\mathbf{v}\|_{\rho^{-1}}} \ge \beta_{\mathsf{D}}, \qquad \inf_{\boldsymbol{\phi}\in\operatorname{Ker}\mathsf{D}} \sup_{\boldsymbol{\psi}\in\mathcal{E}} \frac{[\![\boldsymbol{\phi},\mathsf{C}(\boldsymbol{\psi})]\!]_{\mathcal{F}\tilde{\mathcal{E}}}}{\|\boldsymbol{\phi}\|_{\rho^{-1}}\|\boldsymbol{\psi}\|_{\mu^{-1}}} \ge \beta_{\mathsf{C}}.$$

Proof. To prove the inf-sup condition on D, let $\mathbf{p} \in \widetilde{\mathcal{V}}$ and set $\mathbf{v} := (\mathsf{H}^{\mathcal{F}\tilde{\mathcal{E}}}_{\rho^{-1}})^{-1}(\widetilde{\mathsf{GRAD}}(\mathbf{p}))$. Then, $\mathbf{v} \in \mathcal{F}$, $[\![\mathsf{D}(\mathbf{v}),\mathbf{p}]\!]_{c\tilde{\nu}} = \|\mathbf{v}\|^2_{\rho^{-1}}$, and $\|\widetilde{\mathsf{GRAD}}(\mathbf{p})\|_{2,\widetilde{\mathcal{E}}} \lesssim \|\mathbf{v}\|_{\rho^{-1}}$ owing to mesh regularity and ($\mathbf{A}1$); hence, $\|\mathbf{p}\|_{2,\widetilde{\mathcal{V}}} \lesssim \|\mathbf{v}\|_{\rho^{-1}}$ owing to the discrete Poincaré inequality (51). To prove the inf-sup condition on C, let $\boldsymbol{\phi} \in \operatorname{Ker}\mathsf{D}$. Owing to the exact sequence property (7), there is $\boldsymbol{\psi} \in \mathcal{E}$ s.t. $\boldsymbol{\phi} = \mathsf{CURL}(\boldsymbol{\psi})$; moreover, we can take $\boldsymbol{\psi} \in (\operatorname{Ker}\mathsf{CURL})^{\perp\mathsf{H}}$, the orthogonality being with respect to $\mathsf{H}^{\varepsilon\tilde{\mathcal{F}}}_{\mu^{-1}}$. Then, $[\![\boldsymbol{\phi},\mathsf{C}(\boldsymbol{\psi})]\!]_{\mathcal{F}\tilde{\mathcal{E}}} = \|\boldsymbol{\phi}\|^2_{\rho^{-1}}$ and $\|\boldsymbol{\psi}\|_{2,\mathcal{E}} \lesssim \|\boldsymbol{\phi}\|_{2,\mathcal{F}}$ owing to Lemma 2.2. The norm equivalences on $\mathcal{E}$ and $\mathcal{F}$ conclude the proof. □

A classical consequence of Lemma 4.1 and the fact that A^{cb} is selfadjoint and negative definite is the following [26, Theorem 1]:

Corollary 4.2 (Well-posedness)**.** *Assume ($\mathbf{H}_{\mathrm{M}}$) and ($\mathbf{H}_{\boldsymbol{\Omega}}$). Then, the discrete system* (48) *is well-posed.*

4.3 Error analysis for discrete dual load

Let $(p^*, \underline{\phi}, \underline{\omega}^*)$ solve the 3-field curl formulation (43). Let $(\mathbf{p}^*, \boldsymbol{\phi}, \boldsymbol{\omega}^*)$ solve the discrete system (48). We define the following discrete errors:

$$\boldsymbol{\delta}\mathbf{p}^* := \mathsf{R}_{\widetilde{\mathcal{V}}}(p^*) - \mathbf{p}^*, \quad \boldsymbol{\delta}\boldsymbol{\phi} := \mathsf{R}_{\mathcal{F}}(\underline{\phi}) - \boldsymbol{\phi}, \quad \boldsymbol{\delta}\boldsymbol{\omega}^* := \mathsf{R}_{\mathcal{E}}(\underline{\omega}^*) - \boldsymbol{\omega}^*. \tag{52}$$

Recall the global commuting operators $\lfloor\rho^{-1}, {}_{\mathcal{F}}\tilde{\varepsilon}\rceil(\bullet) := \mathsf{H}^{\mathcal{F}\tilde{\mathcal{E}}}_{\rho^{-1}} \cdot \mathsf{R}_{\mathcal{F}}(\bullet) - \mathsf{R}_{\widetilde{\mathcal{E}}}(\rho^{-1}\bullet)$ and $\lfloor\mu^{-1}, {}_{\varepsilon}\tilde{\mathcal{F}}\rceil(\bullet) := \mathsf{H}^{\varepsilon\tilde{\mathcal{F}}}_{\mu^{-1}} \cdot \mathsf{R}_{\mathcal{E}}(\bullet) - \mathsf{R}_{\widetilde{\mathcal{F}}}(\mu^{-1}\bullet)$. For simplicity, we assume that there are no quadrature errors when evaluating the external load.

Theorem 4.3 (Error bounds with discrete dual load)**.** *Let $(p^*, \underline{\phi}, \underline{\omega}^*)$ solve the 3-field curl formulation* (43) *with homogeneous natural BCs. Let $(\mathbf{p}^*, \boldsymbol{\phi}, \boldsymbol{\omega}^*)$ solve the discrete system* (48) *with the*

discrete dual load $\mathsf{S}_{\mathsf{d}}^{\mathsf{cb}}(\rho, \underline{f}^*)$ *with* $\underline{f}^* \in H^s(\Omega)^3$, $s > 1$. *Assume* ($\mathbf{H}_{\mathrm{M}}$) *and* ($\mathbf{H}_{\boldsymbol{\Omega}}$). *Then, the following error bounds hold:*

$$\|\widetilde{\mathsf{GRAD}}(\boldsymbol{\delta}\mathbf{p}^*)\|_\rho \le \|\lfloor \rho^{-1}, {}_{\mathcal{F}}\tilde{\varepsilon}\rceil(\underline{\mathrm{curl}}\,\underline{\omega}^*)\|_\rho, \tag{53a}$$

$$\|\boldsymbol{\delta}\boldsymbol{\omega}^*\|_{\mu^{-1}} \lesssim \|\lfloor \rho^{-1}, {}_{\mathcal{F}}\tilde{\varepsilon}\rceil(\underline{\mathrm{curl}}\,\underline{\omega}^*)\|_\rho + \|\lfloor \mu^{-1}, {}_{\varepsilon}\tilde{\mathcal{F}}\rceil(\underline{\omega}^*)\|_\mu, \tag{53b}$$

$$\|\boldsymbol{\delta}\boldsymbol{\phi}\|_{\rho^{-1}} \lesssim \|\lfloor \rho^{-1}, {}_{\mathcal{F}}\tilde{\varepsilon}\rceil(\underline{\mathrm{curl}}\,\underline{\omega}^*)\|_\rho + \|\lfloor \mu^{-1}, {}_{\varepsilon}\tilde{\mathcal{F}}\rceil(\underline{\omega}^*)\|_\mu + \|\lfloor \rho^{-1}, {}_{\mathcal{F}}\tilde{\varepsilon}\rceil(\underline{\phi})\|_\rho. \tag{53c}$$

Moreover, if $\underline{\omega}^*, \underline{\mathrm{curl}}(\underline{\omega}^*), \underline{\phi} \in [H^1(\mathrm{C})]^3$ *and* $\underline{\mathrm{curl}}(\underline{f}^*) \in [L^4(\Omega)]^3$, *the following error bounds hold:*

$$\|\widetilde{\mathsf{GRAD}}(\boldsymbol{\delta}\mathbf{p}^*)\|_\rho \lesssim h_{\mathrm{M}} \left(\|\underline{\mathrm{curl}}(\underline{\omega}^*)\|_{[H^1(\mathrm{C})]^3} + \|\underline{\mathrm{curl}}(\underline{f}^*)\|_{[L^4(\Omega)]^3} \right), \tag{54a}$$

$$\|\boldsymbol{\delta}\boldsymbol{\omega}^*\|_{\mu^{-1}} \lesssim h_{\mathrm{M}} \left(\|\underline{\mathrm{curl}}(\underline{\omega}^*)\|_{[H^1(\mathrm{C})]^3} + \|\underline{\mathrm{curl}}(\underline{f}^*)\|_{[L^4(\Omega)]^3} + \|\underline{\omega}^*\|_{[H^1(\mathrm{C})]^3} \right), \tag{54b}$$

$$\|\boldsymbol{\delta}\boldsymbol{\phi}\|_{\rho^{-1}} \lesssim h_{\mathrm{M}} \left(\|\underline{\mathrm{curl}}(\underline{\omega}^*)\|_{[H^1(\mathrm{C})]^3} + \|\underline{\mathrm{curl}}(\underline{f}^*)\|_{[L^4(\Omega)]^3} + \|\underline{\omega}^*\|_{[H^1(\mathrm{C})]^3} + \|\underline{\phi}\|_{[H^1(\mathrm{C})]^3} \right). \tag{54c}$$

Proof. (1) We first derive the error equations. Applying $\mathsf{R}_{\widetilde{\mathcal{F}}}$ to the vorticity definition, $\mathsf{R}_{\widetilde{\mathcal{E}}}$ to the momentum balance, and $\mathsf{R}_{\mathcal{C}}$ to the mass balance in (43) yields

$$\begin{aligned} -\mathsf{R}_{\widetilde{\mathcal{F}}}(\mu^{-1}\underline{\omega}^*) + \widetilde{\mathsf{CURL}}(\mathsf{R}_{\widetilde{\mathcal{E}}}(\rho^{-1}\underline{\phi})) &= 0_{\widetilde{\mathcal{F}}}, \\ \mathsf{R}_{\widetilde{\mathcal{E}}}(\rho^{-1}\,\underline{\mathrm{curl}}(\underline{\omega}^*)) + \widetilde{\mathsf{GRAD}}(\mathsf{R}_{\widetilde{\mathcal{V}}}(p^*)) &= \mathsf{S}_{\mathsf{d}}^{\mathsf{cb}}(\rho, \underline{f}^*), \\ \mathsf{DIV}(\mathsf{R}_{\mathcal{F}}(\underline{\phi})) &= 0_{\mathcal{C}}, \end{aligned}$$

owing to the commuting property (9) on the interior dual mesh entities and the homogeneous BCs (44) on the dual mesh entities touching the boundary $\partial\Omega$. Subtracting from the corresponding equation in (48) and introducing the global commuting operators leads to

$$-\mathsf{H}_{\mu^{-1}}^{\varepsilon\widetilde{\mathcal{F}}}(\boldsymbol{\delta}\boldsymbol{\omega}^*) + \widetilde{\mathsf{CURL}} \cdot \mathsf{H}_{\rho^{-1}}^{\mathcal{F}\widetilde{\varepsilon}}(\boldsymbol{\delta}\boldsymbol{\phi}) = -\lfloor \mu^{-1}, {}_{\varepsilon}\tilde{\mathcal{F}}\rceil(\underline{\omega}^*) + \widetilde{\mathsf{CURL}} \cdot \lfloor \rho^{-1}, {}_{\mathcal{F}}\tilde{\varepsilon}\rceil(\underline{\phi}), \tag{55a}$$

$$\mathsf{H}_{\rho^{-1}}^{\mathcal{F}\widetilde{\varepsilon}} \cdot \mathsf{CURL}(\boldsymbol{\delta}\boldsymbol{\omega}^*) + \widetilde{\mathsf{GRAD}}(\boldsymbol{\delta}\mathbf{p}^*) = \lfloor \rho^{-1}, {}_{\mathcal{F}}\tilde{\varepsilon}\rceil(\underline{\mathrm{curl}}\,\underline{\omega}^*), \tag{55b}$$

$$\mathsf{DIV}(\boldsymbol{\delta}\boldsymbol{\phi}) = 0_{\mathcal{C}}. \tag{55c}$$

(2) Bound on the pressure gradient. We take the duality product of (55b) with $(\mathsf{H}_{\rho^{-1}}^{\mathcal{F}\widetilde{\varepsilon}})^{-1} \cdot \widetilde{\mathsf{GRAD}}(\boldsymbol{\delta}\mathbf{p}^*)$. Proceeding as in Step (2) of the proof of Theorem 3.4 yields (53a).
(3) Bound on the viscous stress circulation. We use the discrete Hodge decomposition (39) based on the discrete Hodge operator $\mathsf{H}_{\mu^{-1}}^{\varepsilon\widetilde{\mathcal{F}}}$. We set $\boldsymbol{\delta}\boldsymbol{\omega}^* = \mathsf{GRAD}(\boldsymbol{\delta}\boldsymbol{\theta}) + \boldsymbol{\delta}\boldsymbol{\omega}_\perp^*$ with $\boldsymbol{\delta}\boldsymbol{\theta} \in \mathcal{V}$ and $\boldsymbol{\delta}\boldsymbol{\omega}_\perp^* \in (\mathrm{Ker}\,\mathsf{CURL})^{\perp\mathsf{H}}$. We take the duality product of (55a) with $\mathsf{GRAD}(\boldsymbol{\delta}\boldsymbol{\theta})$. Observing that $\big[\mathsf{GRAD}(\boldsymbol{\delta}\boldsymbol{\theta}), \widetilde{\mathsf{CURL}}(\mathbf{x})\big]_{\varepsilon\widetilde{\mathcal{F}}} = 0$ for all $\mathbf{x} \in \widetilde{\mathcal{E}}$ and $\big[\!\big[\mathsf{GRAD}(\boldsymbol{\delta}\boldsymbol{\theta}), \mathsf{H}_{\mu^{-1}}^{\varepsilon\widetilde{\mathcal{F}}}(\boldsymbol{\delta}\boldsymbol{\omega}^*)\big]\!\big]_{\varepsilon\widetilde{\mathcal{F}}} = \|\mathsf{GRAD}(\boldsymbol{\delta}\boldsymbol{\theta})\|_{\mu^{-1}}^2$, we infer that $\|\mathsf{GRAD}(\boldsymbol{\delta}\boldsymbol{\theta})\|_{\mu^{-1}} \lesssim \|\lfloor \mu^{-1}, {}_{\varepsilon}\tilde{\mathcal{F}}\rceil(\underline{\omega}^*)\|_\mu$. Then, we take the duality product of (55b) with $\mathsf{CURL}(\boldsymbol{\delta}\boldsymbol{\omega}^*)$. This yields $\|\mathsf{CURL}(\boldsymbol{\delta}\boldsymbol{\omega}^*)\|_{\rho^{-1}} \le \|\lfloor \rho^{-1}, {}_{\mathcal{F}}\tilde{\varepsilon}\rceil(\underline{\mathrm{curl}}\,\underline{\omega}^*)\|_\rho$. Since $\mathsf{CURL}(\boldsymbol{\delta}\boldsymbol{\omega}^*) = \mathsf{CURL}(\boldsymbol{\delta}\boldsymbol{\omega}_\perp^*)$ and $\boldsymbol{\delta}\boldsymbol{\omega}_\perp^* \in (\mathrm{Ker}\,\mathsf{CURL})^{\perp\mathsf{H}}$, we infer from Lemma 2.2 that

$$\|\boldsymbol{\delta}\boldsymbol{\omega}_\perp^*\|_{\mu^{-1}} \lesssim \|\lfloor \rho^{-1}, {}_{\mathcal{F}}\tilde{\varepsilon}\rceil(\underline{\mathrm{curl}}\,\underline{\omega}^*)\|_\rho.$$

Finally, since $\|\boldsymbol{\delta}\boldsymbol{\omega}^*\|_{\mu^{-1}}^2 = \|\mathsf{GRAD}(\boldsymbol{\delta}\boldsymbol{\theta})\|_{\mu^{-1}}^2 + \|\boldsymbol{\delta}\boldsymbol{\omega}_\perp^*\|_{\mu^{-1}}^2$, we infer (53b).
(4) Bound on the mass flux. Owing to (55c), ($\mathbf{H}_{\boldsymbol{\Omega}}$), and (7), there is $\boldsymbol{\delta}\boldsymbol{\psi} \in \mathcal{E}$ s.t. $\boldsymbol{\delta}\boldsymbol{\phi} = \mathsf{CURL}(\boldsymbol{\delta}\boldsymbol{\psi})$, and we can take $\boldsymbol{\delta}\boldsymbol{\psi} \in (\mathrm{Ker}\,\mathsf{CURL})^{\perp\mathsf{H}}$. We take the duality product of (55a) with $\boldsymbol{\delta}\boldsymbol{\psi}$. For the two terms on the left-hand side, we obtain $\big[\!\big[\boldsymbol{\delta}\boldsymbol{\psi}, \mathsf{H}_{\mu^{-1}}^{\varepsilon\widetilde{\mathcal{F}}}(\boldsymbol{\delta}\boldsymbol{\omega}^*)\big]\!\big]_{\varepsilon\widetilde{\mathcal{F}}} \le \|\boldsymbol{\delta}\boldsymbol{\psi}\|_{\mu^{-1}}\|\boldsymbol{\delta}\boldsymbol{\omega}^*\|_{\mu^{-1}}$ and $\big[\!\big[\boldsymbol{\delta}\boldsymbol{\psi}, \widetilde{\mathsf{CURL}} \cdot \mathsf{H}_{\rho^{-1}}^{\mathcal{F}\widetilde{\varepsilon}}(\boldsymbol{\delta}\boldsymbol{\phi})\big]\!\big]_{\varepsilon\widetilde{\mathcal{F}}} = \|\mathsf{CURL}(\boldsymbol{\delta}\boldsymbol{\psi})\|_{\rho^{-1}}^2$. Using Lemma 2.2, Cauchy–Schwarz inequalities, and the previous error bounds leads to (53c).
(5) Finally, the error bounds for smooth solutions result from Lemma 2.3. □

4.4 Error analysis for discrete primal load

Theorem 4.4 (Error bounds with discrete primal load)**.** *Let $(p^*, \phi, \underline{\omega}^*)$ solve the 3-field curl formulation* (43) *with homogeneous natural BCs. Let $(\mathbf{p}^*, \boldsymbol{\phi}, \boldsymbol{\omega}^*)$ solve the discrete system* (48) *with the discrete primal load $\mathsf{S}_{\mathsf{p}}^{\mathsf{cb}}(\rho, \underline{f}^*)$ with $\underline{f}^* \in H^s(\Omega)^3$, $s > \frac{1}{2}$. Assume (**H**$_{\mathrm{M}}$) and (**H**$_{\boldsymbol{\Omega}}$). Then, the following error bounds hold:*

$$\|\widetilde{\mathsf{GRAD}}(\boldsymbol{\delta}\mathbf{p}^*)\|_\rho \le \|\lfloor\rho^{-1}, \tilde{\mathcal{F}\varepsilon}\rceil(\rho\,\underline{\mathrm{grad}}(p^*)\|_\rho, \tag{56a}$$

$$\|\boldsymbol{\delta\omega}^*\|_{\mu^{-1}} \lesssim \|\lfloor\rho^{-1}, \tilde{\mathcal{F}\varepsilon}\rceil(\rho\,\underline{\mathrm{grad}}(p^*))\|_\rho + \|\lfloor\mu^{-1}, \tilde{\varepsilon\mathcal{F}}\rceil(\underline{\omega}^*)\|_\mu, \tag{56b}$$

$$\|\boldsymbol{\delta\phi}\|_{\rho^{-1}} \lesssim \|\lfloor\rho^{-1}, \tilde{\mathcal{F}\varepsilon}\rceil(\rho\,\underline{\mathrm{grad}}(p^*))\|_\rho + \|\lfloor\mu^{-1}, \tilde{\varepsilon\mathcal{F}}\rceil(\underline{\omega}^*)\|_\mu + \|\lfloor\rho^{-1}, \tilde{\mathcal{F}\varepsilon}\rceil(\underline{\phi})\|_\rho. \tag{56c}$$

Moreover, if $\underline{\omega}^*, \underline{\phi}, \underline{\mathrm{grad}}(p^*) \in [H^1(\mathrm{C})]^3$ and $\underline{f}^* \in [L^4(\Omega)]^3$, the following error bounds hold:

$$\|\widetilde{\mathsf{GRAD}}(\boldsymbol{\delta}\mathbf{p}^*)\|_\rho \lesssim h_{\mathrm{M}}\,\|\rho\,\underline{\mathrm{grad}}(p^*)\|_{[H^1(\mathrm{C})]^3}, \tag{57a}$$

$$\|\boldsymbol{\delta\omega}^*\|_{\mu^{-1}} \lesssim h_{\mathrm{M}}\left(\|\rho\,\underline{\mathrm{grad}}(p^*)\|_{[H^1(\mathrm{C})]^3} + \|\underline{\omega}^*\|_{[H^1(\mathrm{C})]^3} + \|\underline{f}^*\|_{[L^4(\Omega)]^3}\right), \tag{57b}$$

$$\|\boldsymbol{\delta\phi}\|_{\rho^{-1}} \lesssim h_{\mathrm{M}}\left(\|\rho\,\underline{\mathrm{grad}}(p^*)\|_{[H^1(\mathrm{C})]^3} + \|\underline{\omega}^*\|_{[H^1(\mathrm{C})]^3} + \|\underline{f}^*\|_{[L^4(\Omega)]^3} + \|\underline{\phi}\|_{[H^1(\mathrm{C})]^3}\right). \tag{57c}$$

Proof. Since $\mathsf{S}_{\mathsf{p}}^{\mathsf{cb}}(\rho, \underline{f}^*) = \mathsf{S}_{\mathsf{d}}^{\mathsf{cb}}(\rho, \underline{f}^*) + \lfloor\rho^{-1}, \tilde{\mathcal{F}\varepsilon}\rceil(\rho\underline{f}^*)$, the main difference with the proof of Theorem 4.3 is that the error equation (55b) is to be replaced by

$$\mathsf{H}_{\rho^{-1}}^{\tilde{\mathcal{F}\varepsilon}} \cdot \mathsf{CURL}(\boldsymbol{\delta\omega}^*) + \widetilde{\mathsf{GRAD}}(\boldsymbol{\delta}\mathbf{p}^*) = -\lfloor\rho^{-1}, \tilde{\mathcal{F}\varepsilon}\rceil(\rho\,\underline{\mathrm{grad}}(p^*)).$$

The rest of the proof follows along similar lines, and is skipped for brevity. □

Remark 4.1 (Comparison with Theorem 4.3). When the divergence-free part of the external load (i.e., $\underline{\mathrm{curl}}(\underline{\omega}^*)$) is expected to dominate over the curl-free part (i.e., $\underline{\mathrm{grad}}(p^*)$), using a discrete primal load is more appropriate since the error bounds do not depend on $\underline{\mathrm{curl}}(\underline{\omega}^*)$. Alternatively, when the curl-free part is expected to dominate over the divergence-free part, using a discrete dual load is more appropriate since the error bounds do not depend on $\underline{\mathrm{grad}}(p^*)$.

5 Numerical Results

We investigate numerically the vertex-based pressure schemes of Section 3 in the case of natural and essential BCs, and for both primal and dual discretizations of the external load. We consider the four combinations: natural (Nat.) BCs & $\mathsf{S}_{\mathsf{p}}^{\mathsf{vb}}(\rho, \underline{f}^*)$, essential (Ess.) BCs & $\mathsf{S}_{\mathsf{p}}^{\mathsf{vb}}(\rho, \underline{f}^*)$, Nat. BCs & $\mathsf{S}_{\mathsf{d}}^{\mathsf{vb}}(\rho, \underline{f}^*)$, and Ess. BCs & $\mathsf{S}_{\mathsf{d}}^{\mathsf{vb}}(\rho, \underline{f}^*)$. The two discrete Hodge operators $\mathsf{H}_\rho^{\varepsilon\tilde{\mathcal{F}}}$ and $\mathsf{H}_\mu^{\mathcal{F}\tilde{\varepsilon}}$ are built using the reconstruction functions from the Discrete Geometric Approach by [19]. The resulting discrete Hodge operators satisfy the stability and $\mathbb{P}_0$-consistency properties (**A**1) and (**A**2); see [11]. The strategy for solving the linear system (30) takes advantage of the CDO framework, which allows us to solve only two SPD systems, since it is possible to operate an exact splitting between pressure and velocity. Applying $\widetilde{\mathsf{DIV}}$ to the momentum equation yields the following SPD system for the pressure:

$$\widetilde{\mathsf{DIV}} \cdot \mathsf{H}_\rho^{\varepsilon\tilde{\mathcal{F}}} \cdot \mathsf{GRAD}(\mathbf{p}^*) = \widetilde{\mathsf{DIV}} \cdot \mathsf{S}^{\mathsf{vb}}(\rho, \underline{f}^*), \tag{58}$$

of size #V which is independent of $\mathbf{u}$. Then, the velocity $\mathbf{u}$ is solved by an augmented Lagrangian approach yielding the following SPD system of size #E, where the right-hand side takes into account the pressure computed in (58):

$$(\mathsf{A}^{\mathsf{vb}} + \lambda \mathsf{B}^{\mathrm{T}} \cdot \mathsf{B})(\mathbf{u}) = \mathsf{S}^{\mathsf{vb}}(\rho, \underline{f}^*) - \mathsf{B}^{\mathrm{T}}(\mathbf{p}^*). \tag{59}$$

Applying $\widetilde{\mathsf{DIV}}$ to this system readily shows that the discrete velocity exactly satisfies both momentum and mass balance in (30). Numerical experiments indicate that a suitable value for the Lagrange multiplier λ is the reciprocal of $\max_{\mathrm{e}\in\mathrm{E}}|\mathfrak{p}_\mathrm{e}|$ with $\mathfrak{p}_\mathrm{e} := \cup_{\mathrm{c}\in\mathrm{C}_\mathrm{e}}\mathfrak{p}_{\mathrm{e},\mathrm{c}}$; see Figure 2.

We consider the system (24) on the unit cube $\Omega = [0,1]^3$ with mass density and viscosity set to 1. The exact pressure and velocity are

$$p(x,y,z) = \sin(2\pi x)\sin(2\pi y)\sin(2\pi z), \qquad \underline{u}(x,y,z) = \begin{bmatrix} \frac{1}{2}\sin(2\pi x)\cos(2\pi y)\cos(2\pi z) \\ \frac{1}{2}\cos(2\pi x)\sin(2\pi y)\cos(2\pi z) \\ -\cos(2\pi x)\cos(2\pi y)\sin(2\pi z) \end{bmatrix}. \tag{60}$$

The external load $\underline{f}^*$ and the BCs are determined from (60). Two sequences of three-dimensional polyhedral meshes of the FVCA6 benchmark [see 28] are tested. The first mesh sequence, labeled PrG, contains prismatic meshes with polygonal basis, and the second sequence, labeled CB, checkerboard meshes, the latter being a classical example of so-called non-matching meshes. Each mesh family consists of successive uniform refinements of an initial mesh. Examples are shown in Figure 5 and quantitative information on the meshes is provided in Table 1.

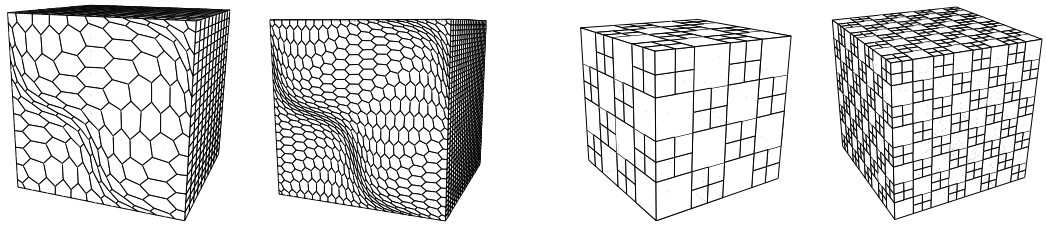

Figure 5: Two examples of prismatic meshes with polygonal basis (left) and of checkerboard meshes (right).

Sequence	Mesh	#V	#E	#F	#C
PrG	coarsest	3 080	7 200	5 331	1 210
	finest	144 320	354 000	276 921	67 240
CB	coarsest	625	1 536	1 200	288
	finest	254 977	700 416	592 896	147 456

Table 1: Cardinality of the mesh entity sets for the coarsest and finest meshes of the PrG and CB mesh sequences

To study the convergence rate of the CDO schemes, we report the following errors:

$$\begin{aligned} \mathrm{Er}_{\mathsf{H}_1}(\mathbf{p}) &:= \frac{\|\mathsf{R}_{\mathcal{V}}(p^*) - \mathbf{p}^*\|_1}{\|\mathsf{R}_{\mathcal{V}}(p^*)\|_1}, \qquad \mathrm{Er}_{\mathsf{H}_\rho}(\mathbf{g}) := \frac{\|\mathsf{R}_{\mathcal{E}}(\underline{\mathrm{grad}}(p^*)) - \mathsf{GRAD}(\mathbf{p}^*)\|_\rho}{\|\mathsf{R}_{\mathcal{E}}(\underline{\mathrm{grad}}(p^*))\|_\rho}, \\ \mathrm{Er}_{\mathsf{H}_\rho}(\mathbf{u}) &:= \frac{\|\mathsf{R}_{\mathcal{E}}(\underline{u}) - \mathbf{u}\|_\rho}{\|\mathsf{R}_{\mathcal{E}}(\underline{u})\|_\rho}, \qquad \mathrm{Er}_{\mathsf{H}_\mu}(\boldsymbol{\omega}) := \frac{\|\mathsf{R}_{\mathcal{E}}(\underline{\mathrm{curl}}\,\underline{u}) - \mathsf{CURL}(\mathbf{u})\|_\mu}{\|\mathsf{R}_{\mathcal{F}}(\underline{\mathrm{curl}}\,\underline{u})\|_\mu}. \end{aligned} \tag{61}$$

The discrete norms $\|\cdot\|_\rho$ and $\|\cdot\|_\mu$ are defined in (27), while $\|\mathbf{a}\|_1^2 := \left[\mathbf{a}, \mathsf{H}_1^{\mathcal{V}\tilde{\mathcal{C}}}(\mathbf{a})\right]_{\mathcal{V}\tilde{\mathcal{C}}} = \|\mathbf{a}\|_{2,\mathcal{V}}^2$, for all $\mathbf{a} \in \mathcal{V}$, with $\mathsf{H}_1^{\mathcal{V}\tilde{\mathcal{C}}}$ defined above Lemma 2.1. The convergence rate R between mesh i and mesh $(i-1)$ within a sequence is defined as

$$\mathrm{R} := -3\frac{\log\left(\mathrm{Er}(i)/\mathrm{Er}(i-1)\right)}{\log\left(\#\mathrm{X}(i)/\#\mathrm{X}(i-1)\right)},$$

where #X is equal to #V for the pressure, #E for the pressure gradient and the velocity, and #F for the vorticity. For the four combinations of BCs and load discretizations, the various errors are plotted in Figure 6 as the meshes are refined, and the observed convergence rates on the finest meshes are

reported in Table 2. The results on the pressure gradient, vorticity, and velocity are in accordance with the theoretical results derived in Section 3. In some cases, some super-convergent behavior is observed. The pressure error appears to converge at second-order for most of the cases considered herein.

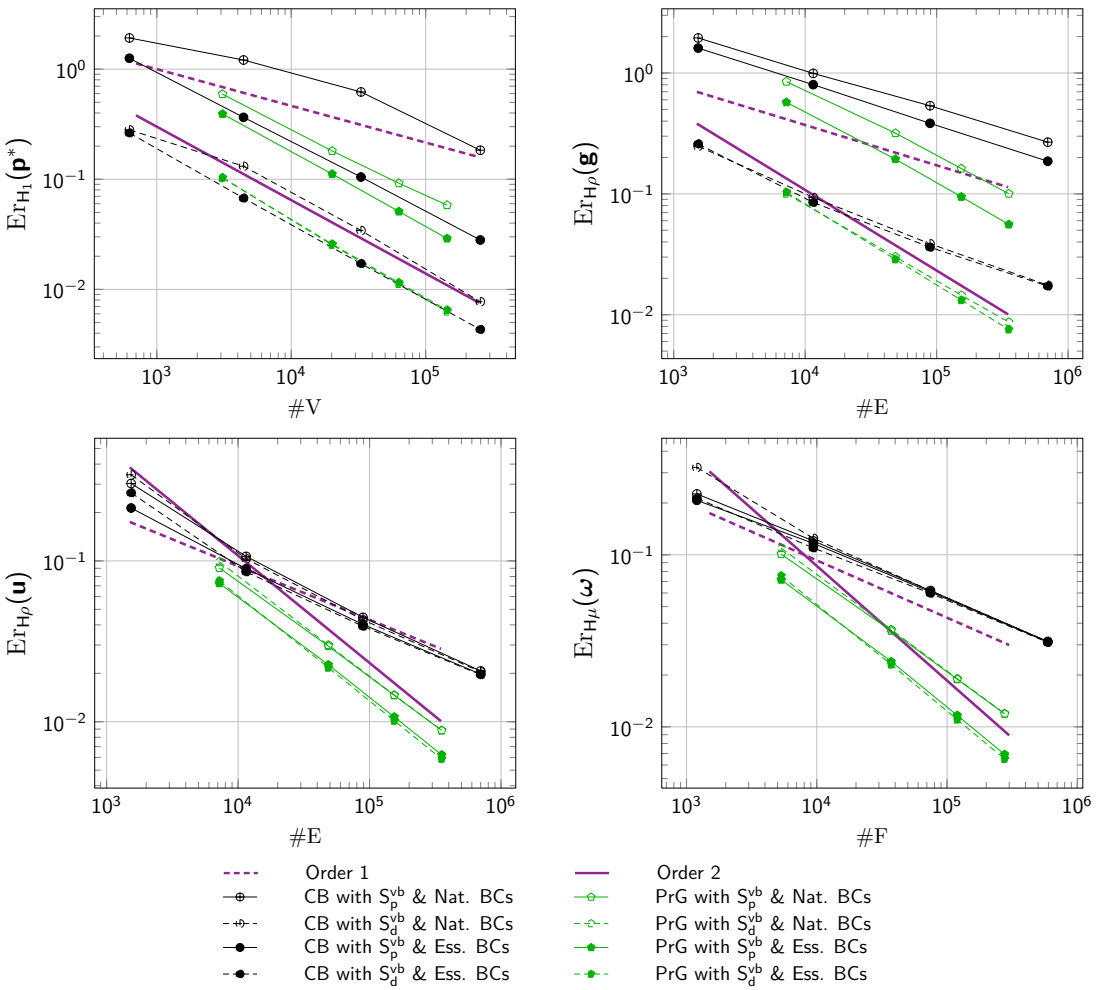

Figure 6: Errors for the two mesh sequences and the four combinations of BCs and load discretization

Finally, we illustrate the practical advantage of the primal and dual load discretizations. We consider the vector potential $\underline{\Psi} = \underline{\mathrm{curl}}(\underline{u})$ and the scalar potential $\Theta = p$ with $\underline{u}$ and p defined in (60), and we take for the external load $\rho \underline{f}^* := \chi_{\underline{u}}\, \underline{\mathrm{curl}}(\underline{\Psi}) + \chi_p\, \underline{\mathrm{grad}}(\Theta)$, with real numbers $\chi_{\underline{u}}$ and χ_p, so that $\rho \underline{f}^*$ has a large curl-free part when $\chi_p \gg 1$ and a large divergence-free part when $\chi_{\underline{u}} \gg 1$. We observe from Figure 7, left, that the discrete pressure error is not affected by the large divergence-free part of the load when choosing a dual discretization. Similarly, we observe from Figure 7, right, that the discrete velocity error is not affected by the large curl-free part of the load when choosing a primal discretization. These numerical results are in agreement with the theoretical results derived in Theorems 3.4 and 3.5. We stress that the Hodge–Helmholtz decomposition of the external load is not used explicitly in the scheme.

			$\mathrm{Er}_{\mathsf{H}_1}(\mathbf{p})$	$\mathrm{Er}_{\mathsf{H}\rho}(\mathbf{g})$	$\mathrm{Er}_{\mathsf{H}\rho}(\mathbf{u})$	$\mathrm{Er}_{\mathsf{H}\mu}(\boldsymbol{\omega})$
PrG	Nat. BCs	$\mathsf{S}_{\mathsf{p}}^{\mathsf{vb}}$	1.7	1.7	1.8	1.7
		$\mathsf{S}_{\mathsf{d}}^{\mathsf{vb}}$	2.1	1.9	1.8	1.7
	Ess. BCs	$\mathsf{S}_{\mathsf{p}}^{\mathsf{vb}}$	2.1	1.9	2.0	1.9
		$\mathsf{S}_{\mathsf{d}}^{\mathsf{vb}}$	2.1	2.0	2.0	1.9
CB	Nat. BCs	$\mathsf{S}_{\mathsf{p}}^{\mathsf{vb}}$	1.8	1.0	1.1	1.0
		$\mathsf{S}_{\mathsf{d}}^{\mathsf{vb}}$	2.2	1.1	1.1	1.0
	Ess. BCs	$\mathsf{S}_{\mathsf{p}}^{\mathsf{vb}}$	1.9	1.1	1.0	1.0
		$\mathsf{S}_{\mathsf{d}}^{\mathsf{vb}}$	2.0	1.1	1.0	0.9

Table 2: Convergence rates between the two finest meshes of each sequence

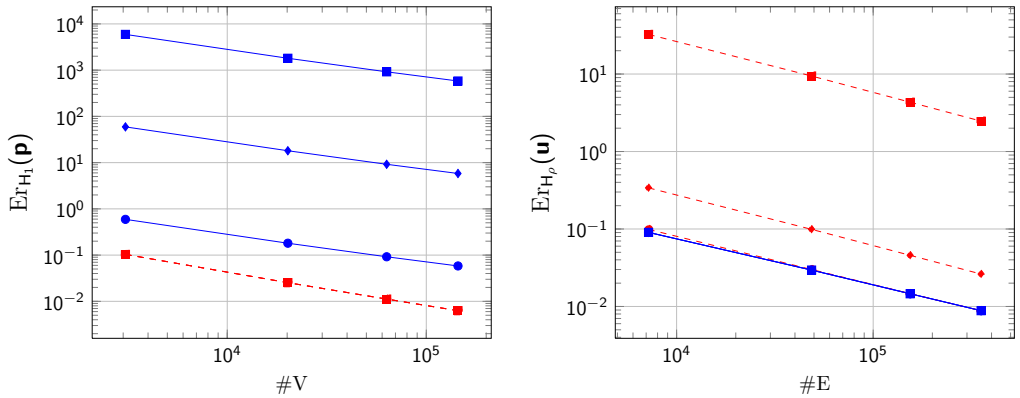

Figure 7: Effect of a primal (blue solid lines) and dual (red dashed lines) discretization of the external load on the sequence of PrG meshes when one considers a large divergence-free part (left) or a large curl-free part (right). Left: Error on the pressure for $\chi_{\underline{u}} \in \{1 \text{ (circle)}, 10^2 \text{ (diamond)}, 10^4 \text{ (square)}\}$ and $\chi_p = 1$; Right: Error on the velocity for $\chi_{\underline{u}} = 1$ and $\chi_p \in \{1 \text{ (circle)}, 10^2 \text{ (diamond)}, 10^4 \text{ (square)}\}$.

6 Conclusions

In this work, we have analyzed CDO schemes for the Stokes equations on three-dimensional polyhedral meshes. The distinction between primal and dual meshes enabled us to devise vertex-based and cell-based pressure schemes. Vertex-based pressure schemes lead to an algebraic system of size (#V + #E) with two unknowns, the pressure located at primal vertices and the velocity at primal edges. Cell-based pressure schemes lead to a system of size (#E + #F + #C) with three unknowns, the pressure located at primal cells, the mass flux at primal faces, and the viscous stress circulation at primal edges. For both schemes, two discrete Hodge operators, related to the mass density and the viscosity, are used; as for elliptic problems, these operators must satisfy a stability and a $\mathbb{P}_0$-consistency property. Both schemes conserve mass and momentum, the vertex-based ones at dual cells and dual faces, respectively, and the cell-based ones at primal cells and dual edges, respectively. Additionally, both schemes can be deployed with two possible load discretizations, so as to handle a large curl-free or divergence-free part of the load.

Various tracks are worth pursuing in future work. The first one is a comparative study of the vertex- and cell-based pressure schemes. Numerical results on elliptic problems [10] show that the computational efficiency of the vertex-based scheme and of the hybridized cell-based scheme is similar, the former leading to a somewhat smaller linear system but with a larger stencil. For elliptic problems, one advantage of the hybrid cell-based schemes is to deliver an exact mass balance on the primal cells (and not the dual ones). For the Stokes equations, a further step in the study of the cell-based pressure scheme is the use of hybridization techniques. Finally, other research tracks include the treatment of essential (and more general) BCs and more general topologies for the domain Ω.

A Proof of discrete Poincaré inequalities

The proof of the discrete Poincaré inequalities hinges on the existence of conforming reconstruction operators $\mathsf{L}_{\mathcal{V}}^{\mathrm{conf}} : \mathcal{V} \to H^1(\Omega)$, $\underline{\mathsf{L}}_{\mathcal{E}}^{\mathrm{conf}} : \mathcal{E} \to H(\underline{\mathrm{curl}};\Omega)$, and $\underline{\mathsf{L}}_{\mathcal{F}}^{\mathrm{conf}} : \mathcal{F} \to H(\mathrm{div};\Omega)$ with right inverse properties $\mathsf{R}_{\mathcal{V}}\mathsf{L}_{\mathcal{V}}^{\mathrm{conf}} = \mathsf{Id}_{\mathcal{V}}$, $\mathsf{R}_{\mathcal{E}}\mathsf{L}_{\mathcal{E}}^{\mathrm{conf}} = \mathsf{Id}_{\mathcal{E}}$, commuting properties $\underline{\mathrm{grad}}(\mathsf{L}_{\mathcal{V}}^{\mathrm{conf}}) = \underline{\mathsf{L}}_{\mathcal{E}}^{\mathrm{conf}}(\mathsf{GRAD})$, $\underline{\mathrm{curl}}(\underline{\mathsf{L}}_{\mathcal{E}}^{\mathrm{conf}}) = \underline{\mathsf{L}}_{\mathcal{F}}^{\mathrm{conf}}(\mathsf{CURL})$, and stability properties $C_{\mathcal{V}}^{\flat}\|\mathbf{p}\|_{2,\mathcal{V}} \le \|\mathsf{L}_{\mathcal{V}}^{\mathrm{conf}}(\mathbf{p})\|_{L^2(\Omega)}$, $\|\mathsf{L}_{\mathcal{E}}^{\mathrm{conf}}(\mathbf{u})\|_{L^2(\Omega)^3} \le C_{\mathcal{E}}^{\sharp}\|\mathbf{u}\|_{2,\mathcal{E}}$, and $\|\mathsf{L}_{\mathcal{F}}^{\mathrm{conf}}(\boldsymbol{\phi})\|_{L^2(\Omega)^3} \le C_{\mathcal{F}}^{\sharp}\|\boldsymbol{\phi}\|_{2,\mathcal{F}}$. One possibility is to use the construction of [17] hinging on local constrained minimization problems using Withney finite elements on the simplicial submesh of each mesh cell. Note that the resulting reconstruction operators are (piecewise) polynomial-valued.

Proof of the discrete Poincaré–Wirtinger inequality. Let $\mathbf{p} \in \mathcal{V}$ be such that $\big[\mathbf{p}, \mathsf{H}_1^{\mathcal{V}\tilde{\mathcal{C}}}(\mathbf{1})\big]_{\mathcal{V}\tilde{\mathcal{C}}} = 0$. Set $z := \mathsf{L}_{\mathcal{V}}^{\mathrm{conf}}(\mathbf{p}) - \langle \mathsf{L}_{\mathcal{V}}^{\mathrm{conf}}(\mathbf{p})\rangle_\Omega \in H^1(\Omega)$ where $\langle\cdot\rangle_\Omega$ denotes the mean-value in Ω. Owing to the continuous Poincaré–Wirtinger inequality, $\|z\|_{L^2(\Omega)} \le C_{\mathrm{P},\Omega}^{(0)}\|\underline{\mathrm{grad}}\, z\|_{L^2(\Omega)^3}$. Moreover, owing to the properties of $\mathsf{L}_{\mathcal{V}}^{\mathrm{conf}}$ and $\underline{\mathsf{L}}_{\mathcal{E}}^{\mathrm{conf}}$, we infer that

$$\|\underline{\mathrm{grad}}\, z\|_{L^2(\Omega)^3} = \|\underline{\mathrm{grad}}(\mathsf{L}_{\mathcal{V}}^{\mathrm{conf}}(\mathbf{p}))\|_{L^2(\Omega)^3} = \|\underline{\mathsf{L}}_{\mathcal{E}}^{\mathrm{conf}}(\mathsf{GRAD}(\mathbf{p}))\|_{L^2(\Omega)^3} \le C_{\mathcal{E}}^{\sharp}\|\mathsf{GRAD}(\mathbf{p})\|_{2,\mathcal{E}},$$

so that $\|z\|_{L^2(\Omega)} \le C_{\mathrm{P},\Omega}^{(0)} C_{\mathcal{E}}^{\sharp}\|\mathsf{GRAD}(\mathbf{p})\|_{2,\mathcal{E}}$. Furthermore, since $\mathbf{p} - \mathsf{R}_{\mathcal{V}}(z) = \langle \mathsf{L}_{\mathcal{V}}^{\mathrm{conf}}(\mathbf{p})\rangle_\Omega \mathbf{1}$, we infer that

$$\|\mathbf{p}\|_{2,\mathcal{V}}^2 = \big[\!\big[\mathbf{p}, \mathsf{H}_1^{\mathcal{V}\tilde{\mathcal{C}}}(\mathbf{p})\big]\!\big]_{\mathcal{V}\tilde{\mathcal{C}}} = \big[\!\big[\mathbf{p}, \mathsf{H}_1^{\mathcal{V}\tilde{\mathcal{C}}}(\mathbf{p} - \mathsf{R}_{\mathcal{V}}(z))\big]\!\big]_{\mathcal{V}\tilde{\mathcal{C}}} + \big[\!\big[\mathbf{p}, \mathsf{H}_1^{\mathcal{V}\tilde{\mathcal{C}}}\mathsf{R}_{\mathcal{V}}(z)\big]\!\big]_{\mathcal{V}\tilde{\mathcal{C}}} = \big[\!\big[\mathbf{p}, \mathsf{H}_1^{\mathcal{V}\tilde{\mathcal{C}}}\mathsf{R}_{\mathcal{V}}(z)\big]\!\big]_{\mathcal{V}\tilde{\mathcal{C}}},$$

so that $\|\mathbf{p}\|_{2,\mathcal{V}} \le \|\mathsf{R}_{\mathcal{V}}(z)\|_{2,\mathcal{V}}$. Finally, since $\|\mathsf{R}_{\mathcal{V}}(z)\|_{2,\mathcal{V}} \le (C_{\mathcal{V}}^{\flat})^{-1}\|\mathsf{L}_{\mathcal{V}}^{\mathrm{conf}}(\mathsf{R}_{\mathcal{V}}(z))\|_{L^2(\Omega)}$ and $\mathsf{L}_{\mathcal{V}}^{\mathrm{conf}}(\mathsf{R}_{\mathcal{V}}(z)) = z$ (observe in particular that $\mathsf{R}_{\mathcal{V}}(1) = \mathbf{1}$ and $\mathsf{L}_{\mathcal{V}}^{\mathrm{conf}}(\mathbf{1}) = 1$), we infer (20) with $C_{\mathrm{P}}^{(0)} = C_{\mathrm{P},\Omega}^{(0)} C_{\mathcal{E}}^{\sharp}(C_{\mathcal{V}}^{\flat})^{-1}$. □

Proof of the discrete Poincaré inequality for the curl. Let $\mathbf{u} \in \mathcal{E}$ be such that $\big[\mathbf{u}, \mathsf{H}_\alpha^{\mathcal{E}\tilde{\mathcal{F}}}(\mathbf{v})\big]_{\mathcal{E}\tilde{\mathcal{F}}} = 0$ for all $\mathbf{v} \in \mathrm{Ker}\,\mathsf{CURL}$. There is $\underline{z} \in H(\underline{\mathrm{curl}};\Omega)$ such that $\underline{\mathrm{curl}}(\underline{z}) = \underline{\mathrm{curl}}(\underline{\mathsf{L}}_{\mathcal{E}}^{\mathrm{conf}}(\mathbf{u}))$ and $\mathrm{div}(\underline{z}) = 0$ in Ω and $\underline{z}\cdot\underline{\nu}_{\partial\Omega} = 0$. For all $\underline{v} \in \mathrm{Ker}\,(\underline{\mathrm{curl}})$, there is $\vartheta \in H^1(\Omega)$ s.t. $\underline{v} = \underline{\mathrm{grad}}(\vartheta)$ owing to $(\mathbf{H_\Omega})$, so that $\int_\Omega \underline{z}\cdot\underline{v} = \int_\Omega \mathrm{div}(\underline{z})\vartheta + \int_{\partial\Omega}(\underline{z}\cdot\underline{\nu}_{\partial\Omega})\vartheta = 0$. Owing to the continuous Poincaré inequality for

the curl, $\|\underline{z}\|_{L^2(\Omega)^3} \le C_{\mathrm{P},\Omega}^{(1)}\|\underline{\mathrm{curl}}(\underline{z})\|_{L^2(\Omega)^3}$. Moreover, owing to [2, Prop. 3.7], there is $s > \frac{1}{2}$ such that $\|\underline{z}\|_{H^s(\Omega)^3} \le C_{H^s}C_{\mathrm{P},\Omega}^{(1)}\|\underline{\mathrm{curl}}(\underline{z})\|_{L^2(\Omega)^3}$. This bound implies that $\underline{z}$ is in the domain of the Nédélec finite element interpolation operator on the simplicial submesh, so that, using mesh regularity, the proof of Prop. 4.6 in the above reference, and the fact that $\underline{\mathrm{curl}}(\underline{z})$ is polynomial-valued, we infer that $\|\!|\mathsf{R}_{\mathcal{E}}(\underline{z})|\!\|_{2,\mathcal{E}} \le C_{\mathrm{N}}C_{H^s}C_{\mathrm{P},\Omega}^{(1)}\|\underline{\mathrm{curl}}(\underline{z})\|_{L^2(\Omega)^3}$. Furthermore, we observe that

$$\big[\!\big[\mathbf{u}, \mathsf{H}_\alpha^{\mathcal{E}\tilde{\mathcal{F}}}(\mathbf{u})\big]\!\big]_{\mathcal{E}\tilde{\mathcal{F}}} = \big[\!\big[\mathbf{u}, \mathsf{H}_\alpha^{\mathcal{E}\tilde{\mathcal{F}}}(\mathbf{u} - \mathsf{R}_{\mathcal{E}}(\underline{z}))\big]\!\big]_{\mathcal{E}\tilde{\mathcal{F}}} + \big[\!\big[\mathbf{u}, \mathsf{H}_\alpha^{\mathcal{E}\tilde{\mathcal{F}}}(\mathsf{R}_{\mathcal{E}}(\underline{z}))\big]\!\big]_{\mathcal{E}\tilde{\mathcal{F}}} = \big[\!\big[\mathbf{u}, \mathsf{H}_\alpha^{\mathcal{E}\tilde{\mathcal{F}}}(\mathsf{R}_{\mathcal{E}}(\underline{z}))\big]\!\big]_{\mathcal{E}\tilde{\mathcal{F}}},$$

since

$$\mathsf{CURL}(\mathbf{u} - \mathsf{R}_{\mathcal{E}}(\underline{z})) = \mathsf{CURL}(\mathsf{R}_{\mathcal{E}}(\underline{\mathsf{L}}_{\mathcal{E}}^{\mathrm{conf}}(\mathbf{u}) - \underline{z})) = \mathsf{R}_{\mathcal{F}}(\underline{\mathrm{curl}}(\underline{\mathsf{L}}_{\mathcal{E}}^{\mathrm{conf}}(\mathbf{u}) - \underline{z})) = 0.$$

Hence, $\|\!|\mathbf{u}|\!\|_\alpha \le \|\!|\mathsf{R}_{\mathcal{E}}(\underline{z})|\!\|_\alpha$, and owing to (**A**1), we infer that

$$\eta_\alpha\|\!|\mathbf{u}|\!\|_{2,\mathcal{E}} \le \|\!|\mathsf{R}_{\mathcal{E}}(\underline{z})|\!\|_{2,\mathcal{E}} \le C_{\mathrm{N}}C_{H^s}C_{\mathrm{P},\Omega}^{(1)}\|\underline{\mathrm{curl}}(\underline{\mathsf{L}}_{\mathcal{E}}^{\mathrm{conf}}(\mathbf{u}))\|_{L^2(\Omega)^3},$$

whence we infer (21) with $C_{\mathrm{P}}^{(1)} = \eta_\alpha^{-1}C_{\mathrm{N}}C_{H^s}C_{\mathrm{P},\Omega}^{(1)}C_{\mathcal{F}}^\sharp$ observing that $\underline{\mathrm{curl}}(\underline{z}) = \underline{\mathrm{curl}}(\underline{\mathsf{L}}_{\mathcal{E}}^{\mathrm{conf}}(\mathbf{u})) = \underline{\mathsf{L}}_{\mathcal{F}}^{\mathrm{conf}}(\mathsf{CURL}(\mathbf{u}))$ and using the stability of $\underline{\mathsf{L}}_{\mathcal{F}}^{\mathrm{conf}}$. □

References

[1] H. Abboud, F. E. Chami, and T. Sayah. A priori and a posteriori estimates for three-dimensional Stokes equations with nonstandard boundary conditions. *Numer. Methods Partial Differential Equations*, 28(4):1178–1193, 2012.

[2] C. Amrouche, C. Bernardi, M. Dauge, and V. Girault. Vector potentials in three-dimensional non-smooth domains. *Math. Meth. Appl. Sci.*, 21(9):823–864, 1998.

[3] B. Andreianov, M. Bendahmane, F. Hubert, and S. Krell. On 3D DDFV discretization of gradient and divergence operators. I. meshing, operators and discrete duality. *IMA Journal of Numerical Analysis*, 32(4):1574–1603, 2012.

[4] D. N. Arnold, R. S. Falk, and R. Winther. Finite Element Exterior Calculus: from Hodge Theory to Numerical Stability. *Bull. Amer. Math. Soc.*, 47:281–354, 2010. DOI: 10.1090/S0273-0979-10-01278-4.

[5] L. Beirão da Veiga, V. Gyrya, K. Lipnikov, and G. Manzini. Mimetic Finite Difference Method for the Stokes Problem on Polygonal Meshes. *Journal of Computational Physics*, 228(19):7215–7232, 2009.

[6] L. Beirão da Veiga, K. Lipnikov, and G. Manzini. Error analysis for mimetic discretization of the steady Stokes problem on polyhedral meshes. *SIAM J. Numer. Anal*, 48(4):1419–1443, 2010.

[7] L. Beirão da Veiga and K. Lipnikov. A mimetic discretization of the Stokes problem with selected edge bubbles. *SIAM J. Sci. Comput.*, 32(2):875–893, 2010.

[8] C. Bernardi and N. Chorfi. Spectral discretization of the vorticity, velocity, and pressure formulation of the Stokes problem. *SIAM J. Numer. Anal*, 44:826–850, 2006.

[9] P. Bochev and J. M. Hyman. Principles of mimetic discretizations of differential operators. In D. Arnold, P. Bochev, R. Lehoucq, R. A. Nicolaides, and M. Shashkov, editors, *Compatible Spatial Discretization*, volume 142 of *The IMA Volumes in mathematics and its applications*, pages 89–120. Springer, 2005.

[10] J. Bonelle. *Compatible Discrete Operator Schemes for Elliptic and Stokes Equations on Polyhedral Meshes*. PhD thesis, University Paris-Est, 2014.

[11] J. Bonelle and A. Ern. Analysis of Compatible Discrete Operator Schemes for Elliptic Problems on Polyhedral Meshes. *ESAIM: Mathematical Modelling and Numerical Analysis*, 48(2):553–581, 2014. DOI:10.1051/m2an/2013104.

[12] A. Bossavit. Computational electromagnetism and geometry. *J. Japan Soc. Appl. Electromagn. & Mech.*, 7-8:150–9 (no 1), 294–301 (no 2), 401–8 (no 3), 102–9 (no 4), 203–9 (no 5), 372–7 (no 6), 1999-2000.

[13] J. H. Bramble and P. Lee. On Variational Formulations for the Stokes Equations with Non-Standard Boundary Conditions. *M2AN Math. Model. Numer. Anal.*, 28(7):903–919, 1994.

[14] F. Brezzi, A. Buffa, and K. Lipnikov. Mimetic Finite Difference for elliptic problem. *Mathematical Modelling and Numerical Analysis*, 43:277–295, 2009.

[15] F. Brezzi and M. Fortin. *Mixed and Hydbrid Finite Element Methods*. Springer series in computational mathematics. Springer-Verlag, 1991.

[16] F. Brezzi, K. Lipnikov, and M. Shashkov. Convergence of the Mimetic Finite Difference method for diffusion problems on polyhedral meshes. *SIAM J. Numer. Anal*, 43(5):1872–1896, 2005.

[17] S. H. Christiansen. A construction of spaces of compatible differential forms on cellular complexes. *Math. Models Methods Appl. Sci.*, 18(5):739–757, 2008.

[18] M. Clemens and T. Weiland. Discrete Electromagnetism with the Finite Integration Technique. *Progress In Electromagnetics Research*, 32:65–87, 2001.

[19] L. Codecasa, R. Specogna, and F. Trevisan. A new set of basis functions for the Discrete Geometric Approach. *Journal of Computational Physics*, 229(19):7401–7410, September 2010.

[20] L. Codecasa and F. Trevisan. Convergence of electromagnetic problems modelled by Discrete Geometric Approach. *CMES*, 58(1):pp. 15–44, 2010.

[21] S. Delcourte and P. Omnes. A Discrete Duality Finite Volume discretization of the vorticity-velocity-pressure formulation of the 2D Stokes problem on almost arbitrary two-dimensional grids. http://hal-cea.archives-ouvertes.fr/cea-00772972, 2013.

[22] M. Desbrun, A. N. Hirani, M. Leok, and J. E. Marsden. Discrete Exterior Calculus. http://arxiv.org/abs/math/0508341, 2005.

[23] D. A. Di Pietro and S. Lemaire. An extension of the Crouzeix-Raviart space to general meshes with application to quasi-incompressible linear elasticity and Stokes flow. *Math. Comp.*, 2014. Accepted for publication.

[24] J. Droniou and R. Eymard. Study of the mixed finite volume method for Stokes and Navier-Stokes equations. *Num. Meth. for Part*, 25(1):137–171, 2009.

[25] F. Dubois. Une formulation tourbillon-vitesse-presion pour le problème de Stokes. *Comptes Rendus de l'Académie des Sciences*, 314:277–280, 1992.

[26] F. Dubois. Vorticity-velocity-pressure formulation for the Stokes problem. *Mathematical Methods in the Applied Sciences*, 25(13):1091–1119, 2002.

[27] R. Eymard, J. Fuhrmann, and A. Linke. On MAC schemes on triangular Delaunay meshes, their convergence and application to coupled flow problems. *Numer. Methods Partial Differential Equations*, 30(4):1397–1424, 2014.

[28] R. Eymard, G. Henry, R. Herbin, F. Hubert, R. Klöfkorn, and G. Manzini. 3D benchmark on discretization schemes for anisotropic diffusion problems on general grids. In *Finite Volumes for Complex Applications VI - Problems & Perspectives*, volume 2, pages 95–130. Springer, 2011.

[29] R. Falk and M. Neilan. Stokes Complexes and the Construction of Stable Finite Elements with Pointwise Mass Conservation. *SIAM J. Numer. Anal*, 51(2):1308–1326, 2013.

[30] M. Gerritsma. An introduction to a compatible spectral discretization method. *Mechanics of Advanced Materials and Structures*, 19(1-3):48–67, 2012.

[31] R. Hiptmair. Discrete Hodge operators: An algebraic perspective. *Progress In Electromagnetics Research*, 32:247–269, 2001.

[32] J. Kreeft and M. Gerritsma. Mixed mimetic spectral element method for Stokes flow: A pointwise divergence-free solution. *Journal of Computational Physics*, 240:284–309, 2013.

[33] S. Krell and G. Manzini. The Discrete Duality Finite Volume method for Stokes equations on three-dimensional polyhedral meshes. *SIAM Journal on Numerical Analysis*, 50, 2012.

[34] Alexander Linke. On the role of the Helmholtz decomposition in mixed methods for incompressible flows and a new variational crime. *Comput. Methods Appl. Mech. Engrg.*, 268:782–800, 2014.

[35] C. Mattiussi. The finite volume, finite element, and finite difference methods as numerical methods for physical field problems. *Advances in Imaging and electron physics*, 113:1–146, 2000.

[36] P. Monk. *Finite Element Methods for Maxwell's Equations*. Numerical Mathematics and Scientific Computation. The Clarendon Press Oxford University Press, 2003.

[37] J. C. Nédélec. Élements Finis Mixtes Incompressibles pour l'Équation de Stokes dans $\mathbb{R}^3$. *Numer. Math.*, 39:97–112, 1982.

[38] J. B. Perot. Discrete Conservation Properties of Unstructured Mesh Schemes. *Annual Review of Fluid Mechanics*, 43(1):299–318, 2011.

[39] J. B. Perot and R. Nallapati. A moving unstructured staggered mesh method for the simulation of incompressible free-surface flows. *Journal of Computational Physics*, 184(1):192–214, 2003.

[40] J. B. Perot and V. Subramanian. Discrete calculus methods for diffusion. *Journal of Computational Physics*, 224(1):59–81, 2007.

[41] T. Tarhasaari, L. Kettunen, and A. Bossavit. Some realizations of a discrete Hodge operator: A reinterpretation of finite element techniques. *IEEE Transactions on magnetics*, 35(3):1494–1497, 1999.

[42] F.L. Teixeira. Differential Forms in Lattice Field Theories: An Overview. *ISRN Mathematical Physics*, 2013:16p, 2013.

[43] E. Tonti. *On the formal structure of physical theories*. Istituto di matematica, Politecnico, Milano, 1975.

[44] E. Tonti. Finite formulation of the electromagnetic field. *Progress In Electromagnetics Research (PIER)*, 32:1–44, 2001.

[45] S. Zaglmayr. *High order finite element methods for electromagnetic field computation*. PhD thesis, Johannes Kepler Universität Linz, 2006.